Measurement of the ratio $\mathcal{B}(t \to Wb)/\mathcal{B}(t \to Wq)$ in pp collisions at $\sqrt{s} = 8$ TeV

CMS Collaboration [*]

CERN, Switzerland

ABSTRACT

The ratio of the top-quark branching fractions $\mathcal{R} = \mathcal{B}(t \to Wb)/\mathcal{B}(t \to Wq)$, where the denominator includes the sum over all down-type quarks ($q = b, s, d$), is measured in the $t\bar{t}$ dilepton final state with proton–proton collision data at $\sqrt{s} = 8$ TeV from an integrated luminosity of 19.7 fb^{-1}, collected with the CMS detector. In order to quantify the purity of the signal sample, the cross section is measured by fitting the observed jet multiplicity, thereby constraining the signal and background contributions. By counting the number of b jets per event, an unconstrained value of $\mathcal{R} = 1.014 \pm 0.003$ (stat.) ± 0.032 (syst.) is measured, in a good agreement with current precision measurements in electroweak and flavour sectors. A lower limit $\mathcal{R} > 0.955$ at the 95% confidence level is obtained after requiring $\mathcal{R} \leq 1$, and a lower limit on the Cabibbo–Kobayashi–Maskawa matrix element $|V_{tb}| > 0.975$ is set at 95% confidence level. The result is combined with a previous CMS measurement of the t-channel single-top-quark cross section to determine the top-quark total decay width, $\Gamma_t = 1.36 \pm 0.02$ (stat.)$^{+0.14}_{-0.11}$ (syst.) GeV.

1. Introduction

Because of its large mass [1], the top quark decays before fragmenting or forming a hadronic bound state [2]. According to the standard model (SM), the top quark decays through an electroweak interaction almost exclusively to an on-shell W boson and a b quark. The magnitude of the top–bottom charged current is proportional to $|V_{tb}|$, an element of the Cabibbo–Kobayashi–Maskawa (CKM) matrix. Under the assumption that the CKM matrix is unitary and given the measured values for V_{ub} and V_{cb} (or V_{ts} and V_{td}), $|V_{tb}|$ is expected to be close to unity and dominate over the off-diagonal elements, i.e. $|V_{tb}| \gg |V_{ts}|, |V_{td}|$. Thus, the decay modes of the top quark to lighter down-type quarks (d or s) are allowed, but highly suppressed. The indirect measurement of $|V_{tb}|$, from the unitarity constraint of the CKM matrix, is $|V_{tb}| = 0.999146^{+0.000021}_{-0.000046}$ [3]. Any deviation from this value or in the partial decay width of the top quark to b quarks, would indicate new physics contributions such as those from new heavy up- and/or down-type quarks or a charged Higgs boson, amongst others [4]. Direct searches at the Large Hadron Collider (LHC) have set lower limits on the mass of these hypothetical new particles [5–15], and the observation of a SM Higgs boson candidate [16–18] places stringent constraints on the existence of a fourth sequential generation of quarks. These results support the validity of both the

unitarity hypothesis and the 3×3 structure of the CKM matrix for the energy scale probed by the LHC experiments. However, other new physics contributions, including those described above, could invalidate the bounds established so far on $|V_{tb}|$ [3].

In this Letter, we present a measurement of $\mathcal{R} = \mathcal{B}(t \to Wb)/\mathcal{B}(t \to Wq)$, where the denominator includes the sum over the branching fractions of the top quark to a W boson and a down-type quark ($q = b, s, d$). Under the assumption of the unitarity of the 3×3 CKM matrix, $\mathcal{R} = |V_{tb}|^2$, and thus to indirectly measure $|V_{tb}|$. In addition, the combination of a determination of $\mathcal{R}$ and a measurement of the t-channel single-top cross section can provide an indirect measurement of the top-quark width (Γ_t) [19]. The most recent measurement of Γ_t based on this approach [20] is found to be compatible with the SM predictions with a relative uncertainty of approximately 22%. The value of $\mathcal{R}$ has been measured at the Tevatron, and the most precise result is obtained by the D0 Collaboration, where $\mathcal{R} = 0.90 \pm 0.04$ (stat. + syst.) [21] indicates a tension with the SM prediction. This tension is enhanced for the measurement in the $t\bar{t}$ dilepton decay channel, where both W bosons decay leptonically and $\mathcal{R} = 0.86^{+0.041}_{-0.042}$ (stat.) ± 0.035 (syst.) is obtained. The most recent measurements by the CDF Collaboration are given in [22,23].

Owing to its purity, the $t\bar{t}$ dilepton channel is chosen for this measurement. Events are selected from the data sample acquired in proton–proton collisions at $\sqrt{s} = 8$ TeV by the Compact Muon Solenoid (CMS) experiment at the LHC during 2012. The integrated luminosity of the analysed data sample is 19.7 ± 0.5 fb^{-1} [24].

The selected events are used to measure the $t\bar{t}$ production cross section by fitting the observed jet multiplicity distribution, constraining the signal and background contributions. The b-quark content of the events is inferred from the distribution of the number of b-tagged jets per event as a function of jet multiplicity for each of the dilepton channels. Data-based strategies are used to constrain the main backgrounds and the contributions of extra jets from gluon radiation in $t\bar{t}$ events. The $\mathcal{R}$ value is measured by fitting the observed b-tagged jet distribution with a parametric model that depends on the observed cross section, correcting for the fraction of jets that cannot be matched to a $t \to Wq$ decay. The model also depends on the efficiency for identifying b jets and discriminating them from other jets. Lastly, the measurement of $\mathcal{R}$ is combined with a previously published CMS result of the t-channel production cross section of single top quarks in pp collisions [25] to yield an indirect determination of the top-quark total decay width.

2. The CMS detector

The central feature of the Compact Muon Solenoid (CMS) apparatus is a superconducting solenoid of 6 m internal diameter, providing a magnetic field of 3.8 T. Within the superconducting solenoid volume are a silicon pixel and strip tracker, a lead tungstate crystal electromagnetic calorimeter (ECAL), and a brass/scintillator hadron calorimeter (HCAL), each composed of a barrel and two endcap sections. Muons are measured in gas-ionisation detectors embedded in the steel flux-return yoke outside the solenoid. Extensive forward calorimetry complements the coverage provided by the barrel and endcap detectors.

The silicon tracker measures charged particles within the pseudorapidity range $|\eta| < 2.5$, where the pseudorapidity η is defined as $\eta = -\ln[\tan(\theta/2)]$ and θ is the polar angle of the trajectory of the particle with respect to the anticlockwise-beam direction. The tracker consists of 1440 silicon pixel and 15 148 silicon strip detector modules and is located in the field of the superconducting solenoid. It provides an impact parameter resolution of $\sim$15 μm and a transverse momentum (p_T) resolution of about 1.5% for 100 GeV particles. The electron energy is measured by the ECAL and its direction is measured by the tracker. The mass resolution for $Z \to ee$ decays is 1.6% when both electrons are in the ECAL barrel, and 2.6% when both electrons are in the ECAL endcap [26]. Matching muons to tracks measured in the silicon tracker results in a p_T resolution between 1 and 10%, for p_T values up to 1 TeV. The jet energy resolution (JER) amounts typically to 15% at 10 GeV, 8% at 100 GeV, and 4% at 1 TeV [27].

A more detailed description of the detector can be found in Ref. [28].

3. Simulation of signal and background events

The top-quark pair production cross section has been calculated at next-to-next-to-leading order (NNLO) and next-to-next-to-leading logarithmic soft gluon terms (NNLL) [29]. In proton–proton collisions at $\sqrt{s} = 8$ TeV, and for a top-quark mass of 172.5 GeV, the expected cross section is $\sigma_{\text{NNLO+NNLL}}(t\bar{t}) = 253^{+6}_{-8}$ (scale) $\pm$ 6 (PDF) pb, where the first uncertainty is from the factorisation and renormalisation scales, and the second is from the parton distribution functions (PDFs). Signal events are simulated for a top-quark mass of 172.5 GeV with the leading-order (LO) Monte Carlo (MC) generator MADGRAPH (v5.1.3.30) [30] matched to PYTHIA (v6.426) [31], where the τ lepton decays are simulated with the TAUOLA package (v27.121.5) [32]. The CTEQ6L1 PDF set is used in the event generation [33]. Matrix elements describing up to three partons, and including b quarks, in addition to the $t\bar{t}$ pair

are included in the generator used to produce the simulated signal samples. An alternative simulation at next-to-leading order (NLO) based on POWHEG (v1.0, r1380) [34–36], using the CTEQ6M PDF set [33] and interfaced with PYTHIA, is used to evaluate the signal description uncertainty. A correction to the simulated top-quark p_T is applied, based on the approximate NNLO computation [37]: the events are reweighted at the generator level to match the top-quark p_T prediction, and the full difference between the reweighted and unweighted simulations is assigned as a systematic uncertainty.

The most relevant background processes for the dilepton channel are from the production of two genuine isolated leptons with large p_T. This includes Drell–Yan (DY) production of charged leptons, i.e. from a Z/γ^* decay, which is modelled with MADGRAPH for dilepton invariant masses above 10 GeV, and is normalised to a NNLO cross section of 4.393 nb, computed using FEWZ [38]. The $Z + \gamma$ process is also simulated with MADGRAPH and normalised to the LO predicted cross section of 123.9 pb. Single-top-quark processes are modelled at NLO with POWHEG [39,40] and normalised to cross sections of 22 ± 2 pb, 86 ± 3 pb, and 5.6 ± 0.2 pb for the tW, t-, and s-channel production, respectively [37]. The theory uncertainties are due to the variation of the PDFs and factorisation and renormalisation scales. Diboson processes are modelled with MADGRAPH and normalised to the NLO cross section computed with MCFM [41]. The generation of WW, WZ, and ZZ pairs is normalised to inclusive cross sections of 54.8 pb, 33.2 pb, and 17.7 pb, respectively. For WZ and ZZ pairs a minimum dilepton invariant mass of 12 GeV is required. Associated production of W or Z bosons with $t\bar{t}$ pairs is modelled with MADGRAPH, and normalised to the LO cross sections of 232 fb and 208 fb, respectively. The production of a W boson in association with jets, which includes misreconstructed and non-prompt leptons, is modelled with MADGRAPH and normalised to a total cross section of 36.3 nb computed with FEWZ. Multijet processes are also studied in simulation but are found to yield negligible contributions to the selected sample.

A detector simulation based on GEANT4 (v.9.4p03) [42,43] is applied after the generator step for both signal and background samples. The presence of multiple interactions (pileup) per bunch crossing is incorporated by simulating additional interactions (both in-time and out-of-time with the collision) with a multiplicity matching that observed in the data. The average number of pileup events in the data is 21 interactions per bunch crossing.

4. Event selection and background determination

The event selection is optimised for $t\bar{t}$ dilepton final states that contain two isolated oppositely charged leptons ℓ (electrons or muons), missing transverse energy (E_T^{miss}) defined below, and at least two jets. Events in which the electrons or muons are from intermediate τ lepton decays are considered as signal events. Dilepton triggers are used to acquire the data samples, where a minimum transverse momentum of 8 GeV is required for each of the leptons, and 17 GeV is required for at least one of the leptons. Electron-based triggers include additional isolation requirements, both in the tracker and calorimeter detectors.

All objects in the events are reconstructed with a particle-flow (PF) algorithm [44,45]. Reconstructed electron and muon candidates are required to have $p_T > 20$ GeV and to be in the fiducial region $|\eta| \leq 2.4$ of the detector. A particle-based relative isolation parameter is computed for each lepton and corrected on an event-by-event basis for the contribution from pileup events. We require that the scalar sum of the p_T of all particle candidates reconstructed in an isolation cone built around the lepton's momentum vector is less than 15% (12%) of the electron (muon) transverse momentum. The isolation cone is defined using the

Table 1

Predicted and observed event yields after the full event selection. The combination of statistical uncertainties with experimental and theoretical systematic uncertainties is reported. Non-dileptonic $t\bar{t}$ channels, identified using a generator-level matching, as well as associated production with vector bosons (W or Z), is designated as "other $t\bar{t}$" and grouped with the expected contribution from single W boson and multijets productions. The expected contribution from vector boson pair processes is designated as "VV".

Source	ee	$\mu\mu$	$e\mu$
$W \to \ell\nu$, multijets, other $t\bar{t}$	134 ± 91	43 ± 10	$(38 \pm 20) \times 10$
VV	292 ± 15	333 ± 16	995 ± 39
$Z/\gamma^* \to \ell\ell$	$(297 \pm 63) \times 10$	$(374 \pm 79) \times 10$	$(184 \pm 39) \times 10$
Single top quark	526 ± 26	583 ± 26	1834 ± 64
$t\bar{t}$ dileptons (signal)	$(1003 \pm 50) \times 10$	$(1104 \pm 54) \times 10$	$(349 \pm 17) \times 10^2$
Total	$(1395 \pm 81) \times 10$	$(1574 \pm 96) \times 10$	$(400 \pm 17) \times 10^2$
Data	13 723	15 596	38 892

radius $R = \sqrt{(\Delta\eta)^2 + (\Delta\phi)^2} = 0.4$, where $\Delta\eta$ and $\Delta\phi$ are the differences in pseudorapidity and azimuthal angle between the particle candidate and the lepton. For each event we require at least two lepton candidates originating from a single primary vertex. Among the vertices identified in the event, the vertex with the largest $\sum p_T^2$, where the sum runs over all tracks associated with the vertex, is chosen as the primary vertex. The two leptons with the highest p_T are chosen to form the dilepton pair. Same-flavour dilepton pairs (ee or $\mu\mu$) compatible with $Z \to \ell\ell$ decays are removed by requiring $|M_Z - M_{\ell\ell}| > 15$ GeV, where M_Z is the Z boson mass [3] and $M_{\ell\ell}$ is the invariant mass of the dilepton system. For all dilepton channels it is further required that $M_{\ell\ell} > 12$ GeV in order to veto low-mass dilepton resonances, and that the leptons have opposite electric charge.

Jets are reconstructed by clustering all the PF candidates using the anti-k_T algorithm [46] with a distance parameter of 0.5. Jet momentum is defined as the vector sum of all particle momenta in the jet, and in the simulation it is found to be within 5 to 10% of the hadron-level momentum over the entire p_T spectrum and detector acceptance. A correction is applied by subtracting the extra energy clustered in jets due to pileup, following the procedure described in Refs. [47,48]. The energies of charged-particle candidates associated with other reconstructed primary vertices in the event are also subtracted. Jet energy scale (JES) corrections are derived from simulation, and are validated with *in-situ* measurements of the energy balance of dijet and photon + jet events [27]. Additional selection criteria are applied to events to remove spurious jet-like features originating from isolated noise patterns in certain HCAL regions. In the selection of $t\bar{t}$ events, at least two jets, each with a corrected transverse momentum $p_T > 30$ GeV and $|\eta| \le 2.4$, are required. The jets must be separated from the selected leptons by $\Delta R(\ell, \text{jet}) = \sqrt{(\Delta\eta)^2 + (\Delta\phi)^2} \ge 0.3$. Events with up to four jets, selected under these criteria, are used.

The magnitude of the vector sum of the transverse momenta of all particles reconstructed in the event is used as the estimator for the momentum imbalance in the transverse plane, E_T^{miss}. All JES corrections applied to the event are also propagated into the E_T^{miss} estimate. For the ee and $\mu\mu$ channels, $E_T^{\text{miss}} > 40$ GeV is required in order to reduce the contamination from lepton pairs produced through the DY mechanism in association with at least two jets.

The DY contribution to the same-flavour dilepton channels is estimated from the data after the full event selection through the modelling of the angle $\Theta_{\ell\ell}$ between the two leptons. The $\Theta_{\ell\ell}$ distribution discriminates between leptons produced in DY processes and leptons from the top-quark pair decay cascade. In the first case an angular correlation is expected, while in the second case the leptons are nearly uncorrelated. The probability distribution function for $\Theta_{\ell\ell}$ is derived from data using a DY-enriched control region selected after inverting the E_T^{miss} requirement of the

standard selection. Studies of simulated events indicate that the shape of the $\Theta_{\ell\ell}$ distribution is well described with this method, and that the contamination from other processes in the control region can be neglected. Compatibility tests performed in simulations using different channels and jet multiplicities are used to estimate an intrinsic 10% uncertainty in the final DY background. The other sources of uncertainty in the method are related to the simulation-based description of the probability distribution function for the $\Theta_{\ell\ell}$ distribution from other processes. Uncertainties are estimated either by propagating the uncertainties in pileup or JES and JER, or by trying alternative functions for the $t\bar{t}$ contribution with varied factorisation/renormalisation scales (μ_R/μ_F) with respect to their nominal values given by the momentum transfer in the event, matrix element/parton shower (ME-PS) matching threshold, or generator choice (POWHEG vs. MADGRAPH). The shapes of kinematic distributions for DY and other processes are used in a maximum-likelihood fit to estimate the amount of DY background in the selected sample. A total uncertainty of 21% is estimated from the data in the rate of DY events for the same-flavour channels.

For the $e\mu$ channel, a similar fit procedure is adopted using a different variable: the transverse mass $M_T = \sqrt{2E_T^{\text{miss}} p_T (1 - \cos\Delta\phi)}$ of each lepton, where $\Delta\phi$ is the difference in azimuthal angle between the lepton and the missing transverse momentum. The distribution of the sum $\sum M_T$ is used as the distribution in the fit. In this case the probability distribution function for $Z/\gamma^* \to \tau\tau \to e\mu$ is derived from simulation. The determination of the uncertainty associated with this method follows a similar prescription to that described above for the same-flavour channels. A total uncertainty of 21% is assigned to the amount of DY contamination in the $e\mu$ channel.

The second-largest background contribution is from single-top-quark processes (in particular the tW channel) that is relevant for this measurement since the decay products of a single top quark (instead of a pair) are selected. The contribution of this process is estimated from simulation. Other background processes are also estimated from simulation. Uncertainties in the normalisation stemming from instrumental uncertainties in the integrated luminosity, trigger and selection efficiencies, and energy scales, as well as generator-specific uncertainties, are taken into account.

Table 1 shows the yields in the data and those predicted for signal and background events after the full event selection. The systematic uncertainties assigned to the predictions of signal and background events include the uncertainties in the JES and JER, pileup modelling, cross section calculations, integrated luminosity, and trigger and selection efficiencies. A conservative uncertainty is assigned to the predicted yields of multijet and $W \to \ell\nu$ background events since these contributions are from misidentified leptons and have been estimated solely from simulation. Good overall

agreement is observed for all three dilepton categories between the yields in data and the sum of expected yields.

5. Cross section measurement

The selected events are categorised by the dilepton channel and the number of observed jets. Fig. 1 shows the expected composition for each event category. Good agreement is observed between the distributions from the data and the expectations, including the control regions, defined as events with fewer than two or more than four jets. The chosen categorisation not only allows one to study the contamination from initial- and final-state gluon radiation (ISR/FSR) in the sample, but also to constrain some of the uncertainties from the data.

The $t\bar{t}$ dilepton signal strength, μ, defined as the ratio of the observed to the expected signal rate, is measured from the jet multiplicity distribution by using a profile likelihood method [49]. A likelihood is calculated from the observed number of events in the k dilepton channels and jet multiplicity categories as

$$\mathcal{L}(\mu, \theta) = \prod_k \mathcal{P}[N_k, \hat{N}_k(\mu, \theta_i)] \cdot \prod_i \rho(\theta_i), \qquad (1)$$

where $\mathcal{P}$ is the Poisson probability density function, N_k is the number of events observed in the k-th category, $\hat{N}_k$ is the total number of expected events from signal and background, and θ_i are the nuisance parameters, distributed according to a probability density function ρ. The nuisance parameters are used to modify the expected number of events according to the different systematic uncertainty sources, which include instrumental effects (such as integrated luminosity, pileup, energy scale and resolution, lepton trigger and selection efficiencies) and signal modelling (μ_R/μ_F, ME-PS scale, top-quark mass, leptonic branching fractions of the W boson) amongst others. The PDF uncertainty is estimated using the PDF4LHC prescription [50,51]. The uncertainty from the choice of the $t\bar{t}$ signal generator is estimated by assigning the difference between the MadGraph-based and the powheg-based predictions as an extra uncertainty in the fit. The nuisance parameters are assumed to be unbiased and distributed according to a log-normal function. Based on the likelihood expressed in Eq. (1), the profile likelihood ratio (PLR) λ is defined as

$$\lambda(\mu) = \frac{\mathcal{L}(\mu, \hat{\hat{\theta}})}{\mathcal{L}(\hat{\mu}, \hat{\theta})}, \qquad (2)$$

where the denominator has estimators $\hat{\mu}$ and $\hat{\theta}$ that maximise the likelihood, and the numerator has estimators $\hat{\hat{\theta}}$ that maximise the likelihood for the specified signal strength μ. The signal strength is obtained after maximising $\lambda(\mu)$ in Eq. (2). This approach allows us to parameterise the effect of the systematic uncertainties in the fit.

The signal strength μ is determined independently in each category, i.e. for each dilepton channel and jet multiplicity. For each category, the purity of the selected sample ($f_{t\bar{t}}$) is defined as the fraction of "true" $t\bar{t}$ signal events in the selected sample, $f_{t\bar{t}} = \mu \cdot N_{t\bar{t}exp}/N_{obs}$, where $N_{t\bar{t}exp}$ is the number of expected $t\bar{t}$ events, and N_{obs} is the total number of observed events. By performing the fit for each category, the purity of the sample is obtained. The results are summarised in Table 2. As expected, the $e\mu$ category has the highest purity ($\approx$90%). Because of the contamination from DY events, the same-flavour channels have lower purity ($\approx$70%). Overall, the signal purity increases with higher jet multiplicity.

As a cross-check, a fit including all categories, gives the range $0.909 < \mu < 1.043$ at the 68% confidence level (CL). This leads to a $t\bar{t}$ production cross section of
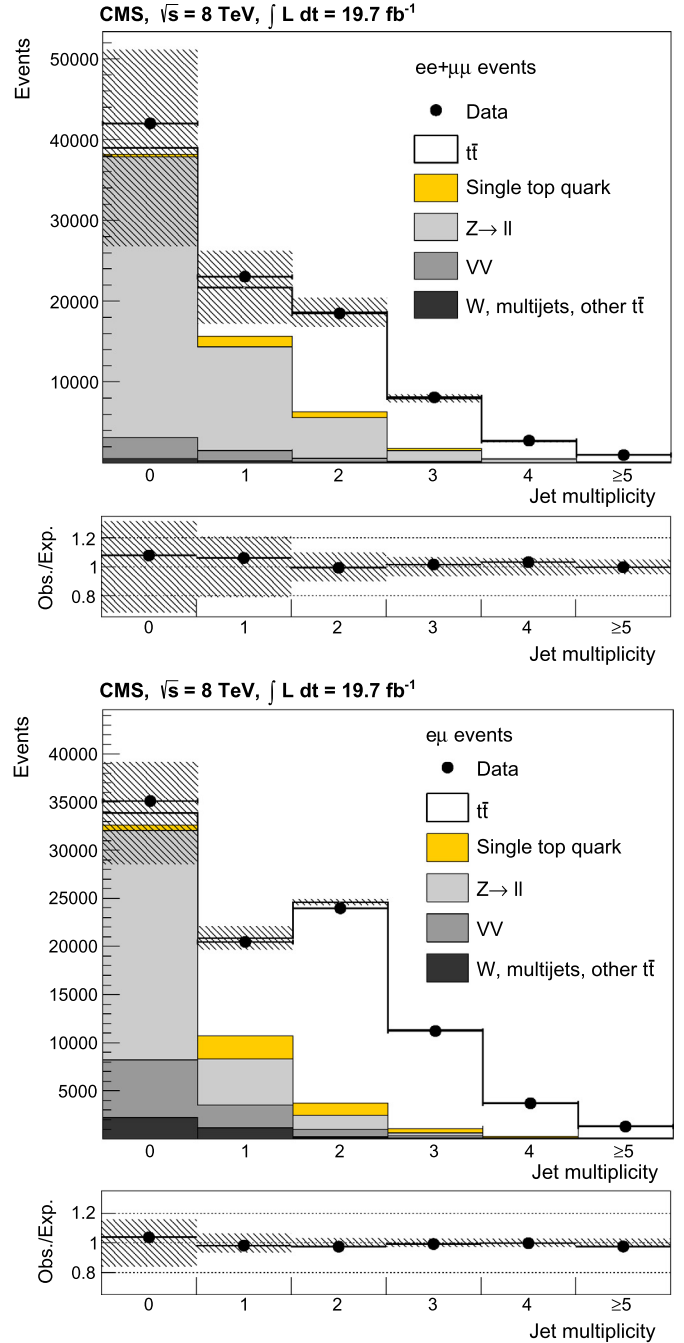
Fig. 1. The upper plots show the observed jet multiplicity after the full event selection, except for the requirement on the number of jets, in the same-flavour (*top*) and different-flavour (*bottom*) channels. The expectations are shown as stacked histograms, while the observed data distributions are represented as closed circles. The predicted distributions for the simulated $t\bar{t}$ and single-top-quark events correspond to a scenario with $\mathcal{R} = 1$. The lower panels show the ratio of the data to the expectations. The shaded bands represent the systematic uncertainty in the determination of the main background (DY) and the integrated luminosity, and vary from 31% (16%) to 5% (3%) in the same- (different-)flavour channels when going from the 0 jets to $\geq$5 jets bin.

$$\sigma(t\bar{t}) = 238 \pm 1 \,(\text{stat.}) \pm 15 \,(\text{syst.}) \text{ pb},$$

in good agreement with NNLO + NNLL expectation [29] and the latest CMS measurement [52]. The result is also found to be consistent with the individual results obtained in each event category. An extra uncertainty is assigned in the extrapolation of the cross section to the full phase space because of the dependence of the
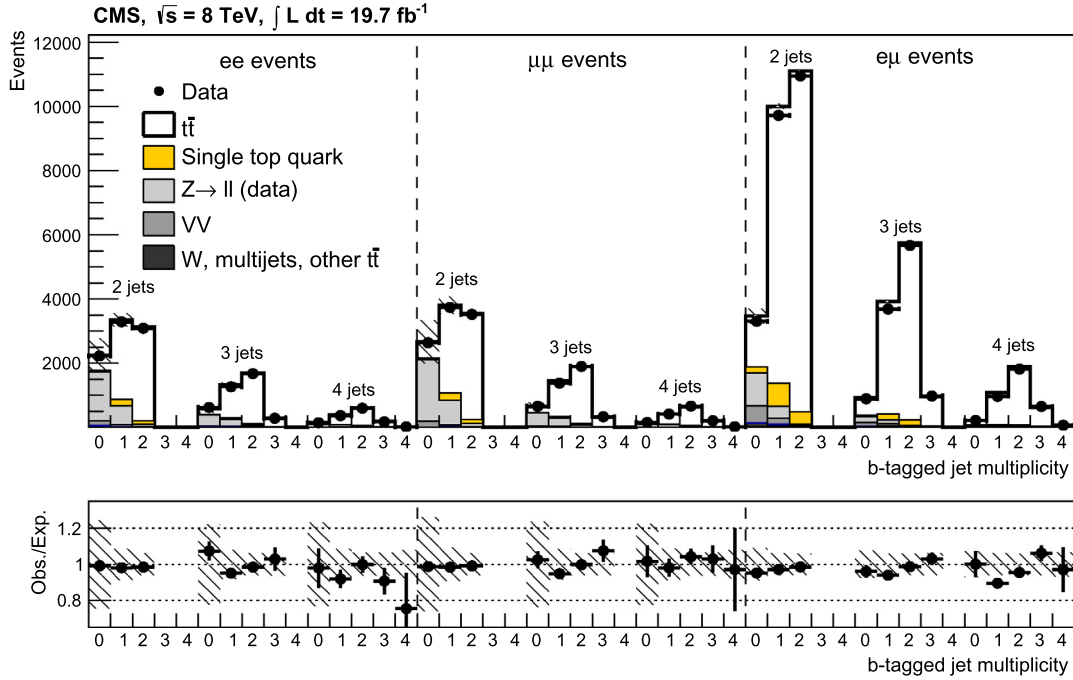
Fig. 2. The upper plot shows the number of b-tagged jets per event for the different $t\bar{t}$ dilepton channels. For each final state, separate subsets are shown corresponding to events with two, three, or four jets. The simulated $t\bar{t}$ and single-top-quark events correspond to a scenario with $\mathcal{R} = 1$. The lower panel shows the ratio of the data to the expectations. The shaded bands represent the uncertainty owing to the finite size of the simulation samples, the main background contribution (DY), and the integrated luminosity.

Table 2

Fraction of $t\bar{t}$ events ($f_{t\bar{t}}$) and relative contribution from single-top-quark processes (k_{st}) for various jet multiplicities and dilepton channels, as determined from the profile likelihood fit. The total uncertainty is shown.

Parameter	Jet multiplicity	Dilepton channel		
		ee	$\mu\mu$	eμ
$f_{t\bar{t}}$	2	0.67 ± 0.07	0.65 ± 0.08	0.85 ± 0.06
	3	0.79 ± 0.06	0.78 ± 0.07	0.90 ± 0.07
	4	0.81 ± 0.11	0.82 ± 0.11	0.94 ± 0.10
k_{st}	2	0.062 ± 0.004	0.063 ± 0.004	0.062 ± 0.003
	3	0.040 ± 0.003	0.040 ± 0.003	0.041 ± 0.002
	4	0.036 ± 0.004	0.036 ± 0.006	0.029 ± 0.003

acceptance on μ_R/μ_F, ME-PS threshold choices, and the top-quark mass.

The relative single-top-quark contribution (k_{st}), defined as the ratio of the expected number of single-top-quark events to the estimated number of inclusive $t\bar{t}$ events, is also shown in Table 2 for each category. For this determination we use the expected number of single-top-quark events obtained after maximising the PLR in Eq. (2). The contribution due to single-top-quark events tends to be most significant in the two-jet category ($<7\%$ relative to inclusive $t\bar{t}$ events). Since the estimate is obtained for a specific scenario in which $\mathcal{R} = 1$, an extra linear dependence of k_{st} on $\mathcal{R}$ is introduced in order to account for the increase in the tW cross section as $|V_{tb}|$ becomes smaller while $|V_{td}|$ and $|V_{ts}|$ become larger [4]. In this parameterisation, the measured ratio $|V_{td}|/|V_{ts}| = 0.211 \pm 0.006$ is used [3], and the uncertainty is considered as an intrinsic systematic uncertainty in the measurement of $\mathcal{R}$.

6. Probing the b-flavour content

In this section the b-flavour content of the selected events (both signal and background) is determined from the b-tagged jet multiplicity distribution. The probability of incorrectly assigning a jet

must be evaluated (Section 6.1) in order to correctly estimate the heavy-flavour content of top-quark decays (Section 6.2).

The b-tagging algorithm that is used (the combined secondary vertex, CSV method described in Ref. [53]) is a multivariate procedure in which both information on the transverse impact parameter with respect to the primary vertex of the associated tracks, and the reconstructed secondary vertices is used to discriminate b jets from c, light-flavour (u, d, s), and gluon jets. The b-tagging efficiency (ε_b) is measured [54] using multijet events where a muon is reconstructed inside a jet; a data-to-simulation scale factor is derived and is used to correct the predicted ε_b value in the $t\bar{t}$ dilepton sample from simulation. After correction, the expected efficiency in the selected $t\bar{t}$ sample is $\approx 84\%$, and the uncertainty in the scale factor from the data is 1–3%, depending on the kinematics of the jets [54]. The same scale factor is applied to the expected c-tagging efficiency but with a doubled uncertainty with respect to the one assigned to b jets owing to the fact that no direct measurement of the c-tagging efficiency is performed. For jets originating from the hadronisation of light-flavour jets, the misidentification efficiency (ε_q) is evaluated [53] from so-called negative tags in jet samples, which are selected using tracks that have a negative impact parameter or secondary vertices with a negative decay length. The scalar product of the jet direction with the vector pointing from the primary vertex to the point of closest approach of a track with negative impact parameter has the opposite sign of the scalar product taken with respect to the point of closest approach. The data-to-simulation correction factor for the misidentification efficiency is known with an uncertainty of about 11%, and the expected misidentification efficiency in the selected sample is approximately 12% [54].

Fig. 2 shows the number of b-tagged jets in the selected dilepton data sample, compared to the expectations from simulation. The multiplicity is shown separately for each dilepton channel and jet multiplicity. The expected event yields are corrected after the PLR fit for the signal strength (described in the previous section)

and also incorporate the data-to-simulation scale factors for ε_b and ε_q. Data and simulation agree within 5%. The residual differences can be related to the different number of jets selected from top-quark decays in data and simulation, the modelling of gluon radiation (ISR/FSR) and if $\mathcal{R}$ is different from unity (which is an assumption used in the simulation).

6.1. Jet misassignment

There is a non-negligible probability that at least one jet from a $t\bar{t}$ decay is missed, either because it falls outside of the detector acceptance or is not reconstructed, and another jet from a radiative process is chosen instead. In the following discussion, this is referred to as a "misassigned jet". Conversely, jets that come from a top-quark decay will be referred to as "correctly assigned". The rate of correct jet assignments is estimated from the data using a combination of three different categories:

- events with no jets selected from top-quark decays, which also include background events with no top quarks;
- events with only one jet from a top-quark decay, which includes some $t\bar{t}$ events and single-top-quark events (mainly produced through the tW channel);
- events with two jets produced from the two top-quark decays.

In order to avoid model uncertainties, the number of selected jets from top-quark decays is derived from the lepton-jet invariant-mass ($M_{\ell j}$) distribution, reconstructed by pairing each lepton with all selected jets. For lepton-jet pairs originating from the same top-quark decay, the endpoint of the spectrum occurs at $M_{\ell j} \approx \sqrt{M_t^2 - M_W^2} \approx 153$ GeV [55], where M_t (M_W) is the top-quark (W boson) mass (Fig. 3, top, open histogram). The predicted distribution for correct pairings is obtained after matching the simulated reconstructed jets to the b quarks from $t \to Wb$ at the generator level using a cone of radius $R = 0.3$. The same quantity calculated for a lepton from a top-quark decay paired with a jet from the top antiquark decay and vice versa ("wrong" pairing) shows a distribution with a long tail (Fig. 3, top, filled histogram), which can be used as a discriminating feature. A similar tail is observed for "unmatched" pairings: either background processes without top quarks, or leptons matched to other jets. The combinations with $M_{\ell j} > 180$ GeV are dominated by incorrectly paired jets, and this control region is used to normalise the contribution from background.

In order to model the lepton-jet invariant-mass distribution of the misassigned jets, an empirical method is used based on the assumption of uncorrelated kinematics. The validity of the method has been tested using simulation. For each event in data, the momentum vector of the selected lepton is "randomly rotated" with uniform probability in the $(\cos(\theta), \phi)$ phase space, and the $M_{\ell j}$ is recomputed. This generates a combinatorial distribution that is used to describe the true distribution of $M_{\ell j}$ for misassigned jets. Fig. 3 (bottom) compares the data distribution with the two components of the $M_{\ell j}$ spectrum, i.e. "correct assignments" from simulation and "wrong assignments" modelled from the data. The background model provides a good estimate of the shape of the spectrum of the misassigned lepton-jet pairs. After fitting the fractions of the two components to the data, the "misassigned" contribution is subtracted from the inclusive spectrum, and the result is compared to the expected contribution from the correctly assigned lepton-jet pairs. The result of this procedure is shown in the inset of Fig. 3 (bottom). This method is used to determine the fraction ($f_{correct}$) of selected jets from top-quark decays in the $M_{\ell j}$ spectrum. Consequently, by measuring $f_{correct}$, we estimate directly
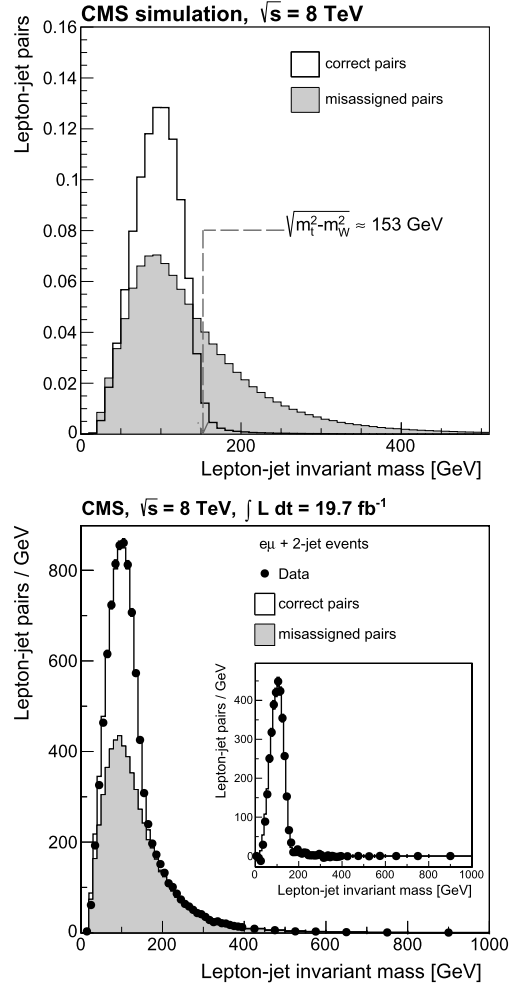
Fig. 3. The top plot shows the correct and misassigned lepton-jet invariant-mass spectra in simulated $t\bar{t}$ dilepton events. Both distributions are normalised to unity. The endpoint of the spectrum for correctly assigned pairs is shown by the dashed line. In the bottom plot the observed data is compared with the correct (from simulation) and misassigned (from the data) components for the lepton-jet invariant-mass spectra in $e\mu$ events with exactly two jets. The lepton-jet mass distribution is shown in the inset, after the misassigned pairs are subtracted.

Table 3
Fraction of lepton-jet pairs correctly assigned in the selected events estimated from the data and predicted from simulation. The last column shows the ratio of the fraction measured in data to the prediction from simulation. The total uncertainty is shown.

Dilepton channel	# jets	$f_{correct}^{data}$	$f_{correct}^{MC}$	data/MC
ee	2	0.28 ± 0.05	0.277 ± 0.001	1.03 ± 0.19
	3	0.22 ± 0.07	0.223 ± 0.001	0.99 ± 0.29
	4	0.19 ± 0.07	0.175 ± 0.001	1.09 ± 0.43
$\mu\mu$	2	0.28 ± 0.06	0.276 ± 0.001	1.00 ± 0.21
	3	0.24 ± 0.06	0.227 ± 0.001	1.05 ± 0.25
	4	0.20 ± 0.07	0.181 ± 0.001	1.08 ± 0.37
$e\mu$	2	0.36 ± 0.06	0.3577 ± 0.0007	1.01 ± 0.16
	3	0.26 ± 0.05	0.2625 ± 0.0007	1.00 ± 0.18
	4	0.21 ± 0.06	0.2047 ± 0.0008	1.00 ± 0.27

from the data the number of top-quark decays reconstructed and selected. Notice that $f_{correct}$ cannot be larger than $1/n$ for events with n jets, as it includes the combinatorial contribution by definition.

In Table 3 the values of $f_{correct}$ found in the data are compared to those predicted from simulation. These include both the
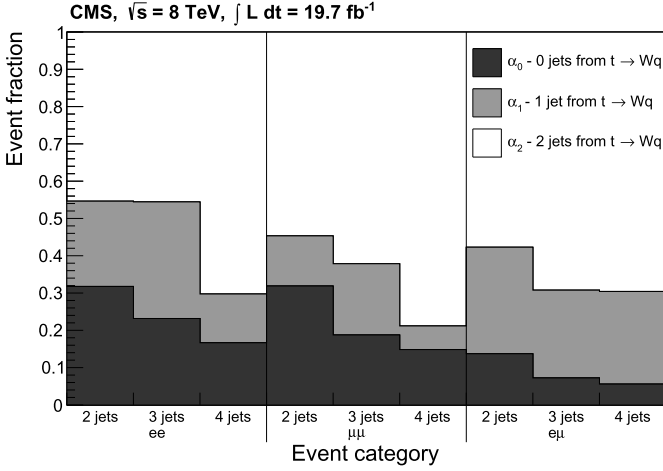
Fig. 4. Fraction of events with 0, 1, or 2 top-quark decays selected, as determined from the data: these fractions, shown for different event categories, are labelled α_0, α_1, and α_2, respectively.

contamination from background events as well as the effect of missing one or two jets from top-quark decays after selection. The systematic uncertainties affecting the estimate of $f_{correct}$ can be split into two sources:

- distortion of the $M_{\ell j}$ shape due to the JES and JER of the reconstructed objects [27];
- calibration uncertainties (derived in the previous section) owing to the uncertainty in the μ_R/μ_F scale, the simulation of gluon radiation and the underlying event, the top-quark mass value used in simulation, and the contributions from background processes.

For each case the fit is repeated with different signal probability distribution functions. The systematic uncertainty is estimated to be 3–10%, depending on the jet multiplicity in the event, and is dominated by the ME-PS matching threshold and the μ_R/μ_F scale uncertainties.

By combining the measured $f_{correct}$ from the data with the fraction of $t\bar{t}$ and single-top-quark events, a parameterisation of the three classes of events is obtained, i.e. the number of events with 0, 1, or 2 selected top-quark decays. The relative amounts of the three event classes are parameterised by the probabilities α_i, where i corresponds to the number of jets from top-quark decays selected in an event. The probabilities α_i are constrained to $\sum_i \alpha_i = 1$. Fig. 4 summarises the values of α_i obtained for the individual event categories, where the differences are dominated by the event selection efficiencies and the background contribution in each category.

6.2. Heavy-flavour content

For a given number of correctly reconstructed and selected jets, the expected b-tagged jet multiplicity can be modelled as a function of $\mathcal{R}$ and the b-tagging and misidentification efficiencies. In the parameterisation, we distinguish events containing jets from 0, 1, or 2 top-quark decays. The model is an extension of the one proposed in Ref. [56]. For illustration, the most significant case is considered, i.e. modelling the observation of two b-tagged jets in an event with two reconstructed jets. For the case where two jets from top-quark decays are selected in the event, the probability to observe two b-tagged jets can be written as

$$P_{2j,2t,2d} = \mathcal{R}^2 \varepsilon_b^2 + 2\mathcal{R}(1-\mathcal{R})\varepsilon_b\varepsilon_q + (1-\mathcal{R})^2 \varepsilon_q^2, \qquad (3)$$

where the subscripts (2j, 2t, 2d) indicate a two-jet event, with two b-tagged jets, and two top-quark decays. If instead, only one jet from a top-quark decay is present in the event, the probability is modified to take the second jet into account in the measurement of $\mathcal{R}$. In this case, the probability of observing two b-tagged jets is

$$P_{2j,2t,1d} = \mathcal{R}^2 \varepsilon_b\varepsilon_{q*} + \mathcal{R}(1-\mathcal{R})(\varepsilon_b + \varepsilon_q)\varepsilon_{q*}$$
$$+ (1-\mathcal{R})^2 \varepsilon_q\varepsilon_{q*}, \qquad (4)$$

where ε_{q*} is the effective misidentification rate, and is computed by taking into account the expected flavour composition of the "extra" jets in the events (i.e. those not matched to a top-quark decay). The effective misidentification rate is derived specifically for each event category. From simulation, these extra jets are expected to come mostly from light-flavour jets ($\approx 87\%$). For completeness, for the case in which no jet from top-quark decay is reconstructed, the probability of observing two b-tagged jets is

$$P_{2j,2t,0d} = \varepsilon_{q*}^2. \qquad (5)$$

For each dilepton channel and jet multiplicity, analogous expressions are derived and combined using the probabilities α_i of having i reconstructed jets from top-quark decays. Additional terms are added to extend the model to events with more than two jets. All efficiencies are determined per event category, after convolving the corrections from dijet events in the data with the expected efficiencies (ε_q and ε_b) and the simulated jet p_T spectrum.

For the measurement of $\mathcal{R}$, a binned-likelihood function is constructed using the model described above and the observed b-tagging multiplicity in events with two, three, or four observed jets in the different dilepton channels. A total of 36 event categories, corresponding to different permutations of three lepton-flavour pairs, three jet multiplicities, and up to four observed b-tagged jets are used (see Fig. 2). The likelihood is generically written as

$$\mathcal{L}(\mathcal{R}, f_{t\bar{t}}, k_{st}, f_{correct}, \varepsilon_b, \varepsilon_q, \varepsilon_{q*}, \theta_i)$$

$$= \prod_{\ell\ell} \prod_{N_{jets}=2...4} \prod_{k=0}^{N_{jets}} \mathcal{P}[N_{ev}^{\ell\ell,N_{jets}}(k), \hat{N}_{ev}^{\ell\ell,N_{jets}}(k)] \prod_i \mathcal{G}(\theta_i^0, \theta_i, 1),$$

$$(6)$$

where $N_{ev}^{\ell\ell,N_{jets}}$ ($\hat{N}_{ev}^{\ell\ell,N_{jets}}$) is the number of observed (expected) events with k b-tagged jets in a given dilepton channel ($\ell\ell =$ ee, $\mu\mu$, eμ) with a given jet multiplicity (N_{jets}), θ_i are the nuisance parameters (a total of 33, which will be discussed later), and $\mathcal{G}$ is a Gaussian distribution. For the nominal fit, the nuisance parameters are assumed to be unbiased ($\theta_i^0 = 0$) and normally distributed. The nuisance parameters parameterise the effect of uncertainties, such as JES and JER, b-tagging and misidentification rates, and μ_R/μ_F scales, amongst others, on the input parameters of the likelihood function. The most likely value for $\mathcal{R}$ is found after profiling the likelihood using the same technique described in Section 5. The result of the fit is verified to be unbiased in simulation, by performing pseudo-experiments with dedicated MC samples where $\mathcal{R}$ is varied in the [0, 1] interval. The residual difference found from these tests is assigned as a model calibration uncertainty.

6.3. Measurement of $\mathcal{R}$

In the fit, $\mathcal{R}$ is allowed to vary without constraints. The parameters of the model are all taken from the data: $f_{t\bar{t}}$ and k_{st} are
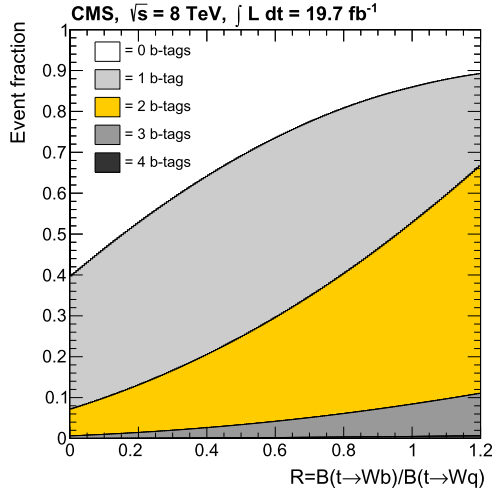
Fig. 5. Expected event fractions of different b-tagged jet multiplicities in dilepton events as a function of $\mathcal{R}$.
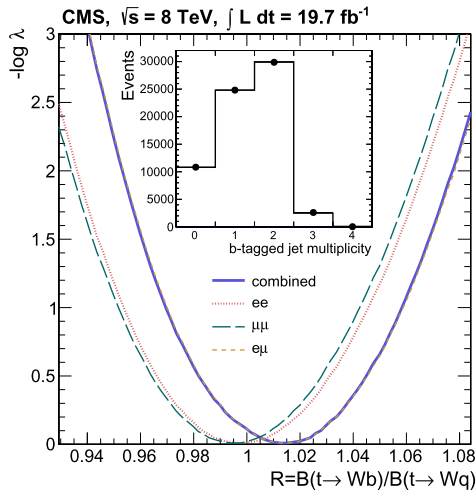

Fig. 6. Variation of the log of the profile likelihood ratio (λ) used to extract $\mathcal{R}$ from the data. The variations observed in the combined fit and in the exclusive ee, $\mu\mu$, and eμ channels, are shown. The inset shows the inclusive b-tagged jet multiplicity distribution and the fit distribution.

taken from Table 2, $f_{correct}$ is taken from Table 3, ε_b and ε_q from dijet-based measurements [53], and ε_{q*} is derived following the method described in the previous section. Fig. 5 shows the resulting prediction for the fraction of events with different numbers of observed b-tagged jets as a function of $\mathcal{R}$. The individual predictions for all categories are summed to build the inclusive model for the observation of up to four b-tagged jets in the selected events.

Fig. 6 shows the results obtained by maximising the profile likelihood. The combined measurement of $\mathcal{R}$ gives $\mathcal{R} = 1.014 \pm 0.003$ (stat.) ± 0.032 (syst.), in good agreement with the SM prediction. Fits to the individual channels give consistent results. For these, we obtain values of $\mathcal{R}_{ee} = 0.997 \pm 0.007$ (stat.) ± 0.035 (syst.), $\mathcal{R}_{\mu\mu} = 0.996 \pm 0.007$ (stat.) ± 0.034 (syst.), and $\mathcal{R}_{e\mu} = 1.015 \pm 0.003$ (stat.) ± 0.031 (syst.) for the ee, $\mu\mu$, and eμ channels, respectively. The measurement in the eμ channel dominates in the final combination since the main systematic uncertainties are fully correlated and this channel has the lowest statistical uncertainty.

The total relative uncertainty in the measurement of $\mathcal{R}$ is 3.2%, and is dominated by the systematic uncertainty, whose individual contributions are summarised in Table 4. The largest contribution

Table 4

Summary of the systematic uncertainties affecting the measurement of $\mathcal{R}$. The values of the uncertainties are relative to the value of $\mathcal{R}$ obtained from the fit.

Source	Uncertainty (%)
Experimental uncertainties:	
ε_b	2.4
ε_q	0.4
$f_{t\bar{t}}$	0.1
DY	0.2
misidentified lepton	0.1
JER	0.5
JES	0.5
unclustered E_T^{miss}	0.5
integrated luminosity	0.2
pileup	0.5
simulation statistics	0.5
$f_{correct}$	0.5
model calibration	0.2
selection efficiency	0.1
Theoretical uncertainties:	
top-quark mass	0.9
top-quark p_T	0.5
ME-PS	0.5
μ_R/μ_F	0.5
signal generator	0.5
underlying event	0.1
colour reconnection	0.1
hadronisation	0.5
PDF	0.1
t → Wq flavour	0.4
$|V_{td}|/|V_{ts}|$	<0.01
relative single-top-quark fraction (tW)	0.1
VV (theoretical cross section)	0.1
extra sources of heavy flavour	0.4
Total systematic	3.2

to the systematic uncertainty is from the b-tagging efficiency measurement. Additional sources of uncertainty are related to the determination of the purity of the sample ($f_{t\bar{t}}$) and the fraction of correct assignments ($f_{correct}$) from the data; these quantities are affected by theoretical uncertainties related to the description of $t\bar{t}$ events, which have similar impact on the final measurement, such as μ_R/μ_F, ME-PS, signal generator, top-quark mass, and top-quark p_T. Instrumental contributions from JES and JER, modelling of the unclustered E_T^{miss} component in simulation, and the contribution from the DY and misidentified-lepton backgrounds are each estimated to contribute a relative systematic uncertainty <0.6%. Another source of uncertainty is due to the contribution from extra sources of heavy-flavour production, either from gluon splitting in radiated jets or from decays in background events such as $W \to c\bar{s}$. This effect has been estimated in the computation of ε_{q*} by assigning a conservative uncertainty of 100% to the c and b contributions. The effect of the uncertainty in the misidentification efficiency is estimated to be small (<1%), as well as other sources of uncertainty, such as pileup and integrated luminosity. After the fit is performed no nuisance parameter is observed to change by more than 1.5σ. The most relevant systematic uncertainty (ε_b) is moved by ~0.5σ as a result of the fit.

If the three-generation CKM matrix is assumed to be unitary, then $\mathcal{R} = |V_{tb}|^2$ [4]. By performing the fit in terms of $|V_{tb}|$, a value of $|V_{tb}| = 1.007 \pm 0.016$ (stat.+syst.) is measured. Upper and lower endpoints of the 95% CL interval for $\mathcal{R}$ are extracted by using the Feldman–Cousins (FC) frequentist approach [57]. The implementation of the FC method in RooStats [58] is used to compute the interval. All the nuisance parameters (including ε_b) are profiled in order to take into account the corresponding uncertainties (statistical and systematic). If the condition $\mathcal{R} \leq 1$ is imposed, we obtain $\mathcal{R} > 0.955$ at the 95% CL. Fig. 7 summarises the expected limit
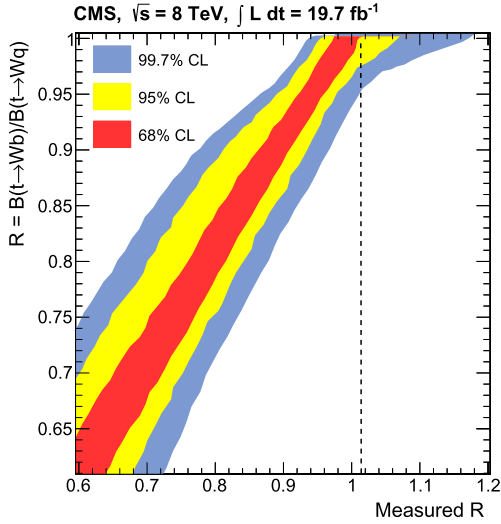
Fig. 7. Expected limit bands at different confidence levels as a function of the measured $\mathcal{R}$ value. The range of measured values of $\mathcal{R}$ that are allowed for each true value of $\mathcal{R}$ is shown as coloured bands for different confidence levels. The observed value of $\mathcal{R}$ is shown as the dashed line.

bands for 68% CL, 95% CL, and 99.7% CL, obtained from the FC method. The expected limit bands are determined from the distribution of the profile likelihood obtained from simulated pseudo-experiments. The upper and lower acceptance regions constructed in this procedure are used to determine the endpoints on the allowed interval for $\mathcal{R}$. In the pseudo-experiments the expected signal and background yields are varied using Poisson probability distributions for the statistical uncertainties and Gaussian distributions for the systematic uncertainties. By constraining $|V_{tb}| \leq 1$, a similar procedure is used to obtain $|V_{tb}| > 0.975$ at the 95% CL.

6.4. Indirect measurement of the top-quark total decay width

The result obtained for $\mathcal{R}$ can be combined with a measurement of the single-top-quark production cross section in the t-channel to yield an indirect determination of the top-quark total width Γ_t. Assuming that $\sum_q \mathcal{B}(t \rightarrow Wq) = 1$, then $\mathcal{R} = \mathcal{B}(t \rightarrow Wb)$ and

$$\Gamma_t = \frac{\sigma_{t\text{-ch.}}}{\mathcal{B}(t \rightarrow Wb)} \cdot \frac{\Gamma(t \rightarrow Wb)}{\sigma_{t\text{-ch.}}^{\text{theor.}}}, \qquad (7)$$

where $\sigma_{t\text{-ch.}}$ ($\sigma_{t\text{-ch.}}^{\text{theor.}}$) is the measured (theoretical) t-channel single-top-quark cross section and $\Gamma(t \rightarrow Wb)$ is the top-quark partial decay width to Wb. If we assume a top-quark mass of 172.5 GeV, then the theoretical partial width of the top quark decaying to Wb is $\Gamma(t \rightarrow Wb) = 1.329$ GeV [3]. A fit to the b-tagged jet multiplicity distribution in the data is performed, leaving Γ_t as a free parameter. In the likelihood function we use the theoretical prediction for the t-channel cross section at $\sqrt{s} = 7$ TeV from Ref. [59] and the corresponding CMS measurement from Ref. [25]. The uncertainties in the predicted and measured cross sections are taken into account as extra nuisance parameters in the fit. The uncertainty in the theoretical cross section is parameterised by convolving a Gaussian function for the PDF uncertainty with a uniform prior describing the factorisation and renormalisation scale uncertainties. Some uncertainties in the experimental cross section measurement such as those from JES and JER, b-tagging efficiency, μ_R/μ_F scales, and ME-PS threshold for $t\bar{t}$ production are fully correlated with the ones assigned to the measurement of $\mathcal{R}$. All others are summed in quadrature and assumed to be uncorrelated. After performing the maximum-likelihood fit, we measure

Table 5
Summary of the systematic uncertainties in the measurement of Γ_t. The values of the uncertainties are relative to the value of Γ_t obtained from the fit. The "other sources" category combines all the individual contributions below 0.5%.

Source	Uncertainty (%)
Single-top quark t-channel cross section	9.2
ε_b	4.3
JES	0.7
pileup	0.8
ME-PS	0.8
μ_R/μ_F	0.8
top-quark mass	0.6
other sources	1.5
Total systematic	10.4

$\Gamma_t = 1.36 \pm 0.02$ (stat.)$^{+0.14}_{-0.11}$ (syst.) GeV, in good agreement with the theoretical expectation [3]. The dominant uncertainty comes from the measurement of the t-channel cross section, as summarised in Table 5.

7. Summary

A measurement of the ratio of the top-quark branching fractions $\mathcal{R} = \mathcal{B}(t \rightarrow Wb)/\mathcal{B}(t \rightarrow Wq)$, where the denominator includes the sum over the branching fractions of the top quark to a W boson and a down-type quark (q = b, s, d), has been performed using a sample of $t\bar{t}$ dilepton events. The sample has been selected from proton–proton collision data at $\sqrt{s} = 8$ TeV from an integrated luminosity of 19.7 fb^{-1}, collected with the CMS detector. The b-tagging and misidentification efficiencies are derived from multijet control samples. The fractions of events with 0, 1, or 2 selected jets from top-quark decays are determined using the lepton-jet invariant-mass spectrum and an empirical model for the misassignment contribution. The unconstrained measured value of $\mathcal{R} = 1.014 \pm 0.003$ (stat.) ± 0.032 (syst.) is consistent with the SM prediction, and the main systematic uncertainty is from the b-tagging efficiency ($\approx 2.4\%$). All other uncertainties are $<1\%$. A lower limit of $\mathcal{R} > 0.955$ at 95% CL is obtained after requiring $\mathcal{R} \leq 1$ and taking into account both statistical and systematical uncertainties. This result translates into a lower limit $|V_{tb}| > 0.975$ at 95% CL when assuming the unitarity of the three-generation CKM matrix. By combining this result with a previous CMS measurement of the t-channel production cross section for single top quarks, an indirect measurement of the top-quark total decay width $\Gamma_t = 1.36 \pm 0.02$ (stat.)$^{+0.14}_{-0.11}$ (syst.) GeV is obtained, in agreement with the SM expectation. These measurements of $\mathcal{R}$ and Γ_t are the most precise to date and the first obtained at the LHC.

Acknowledgements

References

[1] ATLAS Collaboration, CDF Collaboration, CMS Collaboration, D0 Collaboration, First combination of Tevatron and LHC measurements of the top-quark mass, LHC-Tevatron Note: ATLAS-CONF-2014-008, CDF-NOTE-11071, CMS-PAS-TOP-13-014, D0-NOTE-6416, 2014, cds.cern.ch/record/1669819, arXiv:1403.4427.

[2] I.I. Bigi, Weak decays of heavy flavors: a phenomenological update, Phys. Lett. B 169 (1986) 101, http://dx.doi.org/10.1016/0370-2693(86)90694-5.

[3] J. Beringer, et al., Particle Data Group, Review of particle physics, Phys. Rev. D 86 (2012) 010001, http://dx.doi.org/10.1103/PhysRevD.86.010001.

[4] J. Alwall, R. Frederix, J.-M. Gérard, A. Giammanco, M. Herquet, S. Kalinin, E. Kou, V. Lemaitre, F. Maltoni, Is $V_{tb} \simeq 1$?, Eur. Phys. J. C 49 (2007) 791, http://dx.doi.org/10.1140/epjc/s10052-006-0137-y, arXiv:hep-ph/0607115.

[5] S. Chatrchyan, et al., CMS Collaboration, Search for heavy bottom-like quarks in 4.9 fb^{-1} of pp collisions at $\sqrt{s} = 7$ TeV, JHEP 05 (2012) 123, http://dx.doi.org/10.1007/JHEP05(2012)123, arXiv:1204.1088.

[6] S. Chatrchyan, et al., CMS Collaboration, Combined search for the quarks of a sequential fourth generation, Phys. Rev. D 86 (2012) 112003, http://dx.doi.org/10.1103/PhysRevD.86.112003, arXiv:1209.1062.

[7] Search for pair-produced heavy quarks decaying to Wq in the two-lepton channel at $\sqrt{s} = 7$ TeV with the ATLAS detector, Phys. Rev. D 86 (2012) 012007, http://dx.doi.org/10.1103/PhysRevD.86.012007, arXiv:1202.3389.

[8] CMS Collaboration, Search for heavy, top-like quark pair production in the dilepton final state in pp collisions at $\sqrt{s} = 7$ TeV, Phys. Lett. B 716 (2012) 103, http://dx.doi.org/10.1016/j.physletb.2012.07.059, arXiv:1203.5410.

[9] Search for pair production of heavy top-like quarks decaying to a high-p_T W boson and a b quark in the lepton plus jets final state at $\sqrt{s} = 7$ TeV with the ATLAS detector, Phys. Lett. B 718 (2013) 1284, http://dx.doi.org/10.1016/j.physletb.2012.11.071, arXiv:1210.5468.

[10] Search for pair production of a new quark that decays to a Z boson and a bottom quark with the ATLAS detector, Phys. Rev. Lett. 109 (2012) 071801, http://dx.doi.org/10.1103/PhysRevLett.109.071801, arXiv:1204.1265.

[11] CMS Collaboration, Inclusive search for a vector-like T quark with charge 2/3 in pp collisions at $\sqrt{s} = 8$ TeV, Phys. Lett. B 729 (2014) 149, http://dx.doi.org/10.1016/j.physletb.2014.01.006, arXiv:1311.7667.

[12] S. Chatrchyan, et al., CMS Collaboration, Search for top-quark partners with charge 5/3 in the same-sign dilepton final state, Phys. Rev. Lett. 112 (2014) 171801, arXiv:1312.2391.

[13] CMS Collaboration, Search for a light charged Higgs boson in top quark decays in pp collisions at $\sqrt{s} = 7$ TeV, JHEP 07 (2012) 143, http://dx.doi.org/10.1007/JHEP07(2012)143, arXiv:1205.5736.

[14] Search for a light charged Higgs boson in the decay channel $H^+ \to c\bar{s}$ in $t\bar{t}$ events using pp collisions at $\sqrt{s} = 7$ TeV with the ATLAS detector, Eur. Phys. J. C 73 (2013) 2465, http://dx.doi.org/10.1140/epjc/s10052-013-2465-z, arXiv:1302.3694.

[15] ATLAS Collaboration, Search for charged Higgs bosons through the violation of lepton universality in $t\bar{t}$ events using pp collision data at $\sqrt{s} = 7$ TeV

[16] with the ATLAS experiment, JHEP 03 (2013) 076, http://dx.doi.org/10.1007/JHEP03(2013)076, arXiv:1212.3572.

[16] ATLAS Collaboration, Observation of a new particle in the search for the Standard Model Higgs boson with the ATLAS detector at the LHC, Phys. Lett. B 716 (2012) 1, http://dx.doi.org/10.1016/j.physletb.2012.08.020, arXiv:1207.7214.

[17] CMS Collaboration, Observation of a new boson at a mass of 125 GeV with the CMS experiment at the LHC, Phys. Lett. B 716 (2012) 30, http://dx.doi.org/10.1016/j.physletb.2012.08.021, arXiv:1207.7235.

[18] S. Chatrchyan, et al., CMS Collaboration, Observation of a new boson with mass near 125 GeV in pp collisions at $\sqrt{s} = 7$ and 8 TeV, JHEP 06 (2013) 081, http://dx.doi.org/10.1007/JHEP06(2013)081, arXiv:1303.4571.

[19] C.P. Yuan, A new method to detect a heavy top quark at the Tevatron, Phys. Rev. D 41 (1990) 42, http://dx.doi.org/10.1103/PhysRevD.41.42.

[20] V.M. Abazov, et al., D0 Collaboration, An improved determination of the width of the top quark, Phys. Rev. D 85 (2012) 091104, http://dx.doi.org/10.1103/PhysRevD.85.091104, arXiv:1201.4156.

[21] V.M. Abazov, et al., D0 Collaboration, Precision measurement of the ratio $\mathcal{B}(t \to Wb)/\mathcal{B}(t \to Wq)$, Phys. Rev. Lett. 107 (2011) 121802, http://dx.doi.org/10.1103/PhysRevLett.107.121802, arXiv:1106.5436.

[22] T. Aaltonen, et al., CDF Collaboration, Measurement of $R = \mathcal{B}(t \to Wb)/\mathcal{B}(t \to Wq)$ in top quark pair decays using lepton + jets events and the full CDF Run II data set, Phys. Rev. D 87 (2013) 111101, http://dx.doi.org/10.1103/PhysRevD.87.111101, arXiv:1303.6142.

[23] T. Aaltonen, et al., CDF Collaboration, Measurement of $R = \mathcal{B}(t \to Wb)/\mathcal{B}(t \to Wq)$ in top-quark-pair decays using dilepton events and the full CDF Run II data set, Phys. Rev. Lett. 112 (2014) 221801, http://dx.doi.org/10.1103/PhysRevLett.112.221801, arXiv:1404.3392.

[24] CMS Collaboration, CMS luminosity based on pixel cluster counting – Summer 2013 Update, CMS Physics Analysis Summary CMS-PAS-LUM-13-001, 2013, http://cds.cern.ch/record/1598864.

[25] CMS Collaboration, Measurement of the single-top-quark t-channel cross section in pp collisions at $\sqrt{s} = 7$ TeV, JHEP 12 (2012) 035, http://dx.doi.org/10.1007/JHEP12(2012)035, arXiv:1209.4533.

[26] CMS Collaboration, Energy calibration and resolution of the CMS electromagnetic calorimeter in pp collisions at $\sqrt{s} = 7$ TeV, J. Instrum. 8 (2013) P09009, http://dx.doi.org/10.1088/1748-0221/8/09/P09009, arXiv:1306.2016.

[27] CMS Collaboration, Determination of jet energy calibration and transverse momentum resolution in CMS, J. Instrum. 6 (2011) P11002, http://dx.doi.org/10.1088/1748-0221/6/11/P11002, arXiv:1107.4277.

[28] CMS Collaboration, The CMS experiment at the CERN LHC, J. Instrum. 3 (2008) S08004, http://dx.doi.org/10.1088/1748-0221/3/08/S08004.

[29] M. Czakon, P. Fiedler, A. Mitov, The total top quark pair production cross section at hadron colliders through $\mathcal{O}(\alpha_S^4)$, Phys. Rev. Lett. 110 (2013) 252004, http://dx.doi.org/10.1103/PhysRevLett.110.252004, arXiv:1303.6254.

[30] J. Alwall, M. Herquet, F. Maltoni, O. Mattelaer, T. Stelzer, MadGraph 5: going beyond, JHEP 06 (2011) 128, http://dx.doi.org/10.1007/JHEP06(2011)128, arXiv:1106.0522.

[31] T. Sjöstrand, S. Mrenna, P.Z. Skands, PYTHIA 6.4 physics and manual, JHEP 05 (2006) 026, http://dx.doi.org/10.1088/1126-6708/2006/05/026, arXiv:hep-ph/0603175.

[32] N. Davidson, G. Nanava, T. Przedziński, E. Richter-Wąs, Z. Wąs, Universal interface of TAUOLA technical and physics documentation, Comput. Phys. Commun. 183 (2012) 821, http://dx.doi.org/10.1016/j.cpc.2011.12.009, arXiv:1002.0543.

[33] J. Pumplin, D.R. Stump, J. Huston, H.-L. Lai, P. Nadolsky, W.-K. Tung, New generation of parton distributions with uncertainties from global QCD analysis, JHEP 07 (2002) 012, http://dx.doi.org/10.1088/1126-6708/2002/07/012, arXiv:hep-ph/0201195.

[34] P. Nason, A new method for combining NLO QCD with shower Monte Carlo algorithms, JHEP 11 (2004) 040, http://dx.doi.org/10.1088/1126-6708/2004/11/040, arXiv:hep-ph/0409146.

[35] S. Frixione, P. Nason, C. Oleari, Matching NLO QCD computations with parton shower simulations: the POWHEG method, JHEP 11 (2007) 070, http://dx.doi.org/10.1088/1126-6708/2007/11/070, arXiv:0709.2092.

[36] S. Alioli, P. Nason, C. Oleari, E. Re, A general framework for implementing NLO calculations in shower Monte Carlo programs: the POWHEG BOX, JHEP 06 (2010) 043, http://dx.doi.org/10.1007/JHEP06(2010)043, arXiv:1002.2581.

[37] N. Kidonakis, Differential and total cross sections for top pair and single top production, in: XX International Workshop on Deep-Inelastic Scattering and Related Subjects, 2012, p. 831, arXiv:1205.3453, an update can be found in arXiv:1311.0283.

[38] K. Melnikov, F. Petriello, Electroweak gauge boson production at hadron colliders through $\mathcal{O}(\alpha_S^2)$, Phys. Rev. D 74 (2006) 114017, http://dx.doi.org/10.1103/PhysRevD.74.114017, arXiv:hep-ph/0609070.

[39] S. Alioli, P. Nason, C. Oleari, E. Re, NLO single-top production matched with shower in POWHEG: s- and t-channel contributions, JHEP 09 (2009) 111, http://dx.doi.org/10.1088/1126-6708/2009/09/111, arXiv:0907.4076; http://dx.doi.org/10.1007/JHEP02(2010)011 (Erratum).

[40] E. Re, Single-top Wt-channel production matched with parton showers using the POWHEG method, Eur. Phys. J. C 71 (2011) 1547, http://dx.doi.org/10.1140/epjc/s10052-011-1547-z, arXiv:1009.2450.

[41] J.M. Campbell, R.K. Ellis, MCFM for the Tevatron and the LHC, Nucl. Phys. B, Proc. Suppl. 205 (2010) 10, http://dx.doi.org/10.1016/j.nuclphysbps.2010.08.011, arXiv:1007.3492.

[42] J. Allison, et al., GEANT4 developments and applications, IEEE Trans. Nucl. Sci. 53 (2006) 270, http://dx.doi.org/10.1109/TNS.2006.869826.

[43] S. Agostinelli, et al., Geant4 Collaboration, GEANT4—a simulation toolkit, Nucl. Instrum. Methods Phys. Res., Sect. A 506 (2003) 250, http://dx.doi.org/10.1016/S0168-9002(03)01368-8.

[44] CMS Collaboration, Particle flow event reconstruction in CMS and performance for jets, taus, and $E_{\mathrm{T}}^{\mathrm{miss}}$, CMS Physics Analysis Summary CMS-PAS-PFT-09-001, 2009, http://cdsweb.cern.ch/record/1194487.

[45] CMS Collaboration, Commissioning of the particle flow event reconstruction with the first LHC collisions recorded in the CMS detector, CMS Physics Analysis Summary CMS-PAS-PFT-10-001, 2010, http://cdsweb.cern.ch/record/1247373.

[46] M. Cacciari, G.P. Salam, G. Soyez, The anti-k_t jet clustering algorithm, JHEP 04 (2008) 063, http://dx.doi.org/10.1088/1126-6708/2008/04/063, arXiv:0802.1189.

[47] M. Cacciari, G.P. Salam, G. Soyez, The catchment area of jets, JHEP 04 (2008) 005, http://dx.doi.org/10.1088/1126-6708/2008/04/05, arXiv:0802.1188.

[48] M. Cacciari, G.P. Salam, Pileup subtraction using jet areas, Phys. Lett. B 659 (2008) 119, http://dx.doi.org/10.1016/j.physletb.2007.09.077, arXiv:0707.1378.

[49] G. Cowan, K. Cranmer, E. Gross, O. Vitells, Asymptotic formulae for likelihood-based tests of new physics, Eur. Phys. J. C 71 (2011) 1554, http://dx.doi.org/10.1140/epjc/s10052-011-1554-0, arXiv:1007.1727.

[50] S. Alekhin, et al., The PDF4LHC Working Group Interim Report, arXiv:1101.0536, 2011.

[51] M. Botje, J. Butterworth, A. Cooper-Sarkar, A. de Roeck, J. Feltesse, S. Forte, A. Glazov, J. Huston, R. McNulty, T. Sjöstrand, R.S. Thorne, The PDF4LHC Working Group Interim Recommendations, arXiv:1101.0538, 2011.

[52] CMS Collaboration, Measurement of the $t\bar{t}$ production cross section in the dilepton channel in pp collisions at $\sqrt{s} = 8$ TeV, JHEP 02 (2014) 024, http://dx.doi.org/10.1007/JHEP02(2014)024, arXiv:1312.7582.

[53] CMS Collaboration, Identification of b-quark jets with the CMS experiment, J. Instrum. 8 (2013) P04013, http://dx.doi.org/10.1088/1748-0221/8/04/P04013, arXiv:1211.4462.

[54] CMS Collaboration, Performance of b tagging at $\sqrt{s} = 8$ TeV in multijet, $t\bar{t}$ and boosted topology events, CMS Physics Analysis Summary CMS-PAS-BTV-13-001, 2012, http://cds.cern.ch/record/1581306.

[55] R.K. Ellis, W.J. Stirling, B.R. Webber, QCD and Collider Physics, Cambridge University Press, 1996.

[56] P. Silva, M. Gallinaro, Probing the flavor of the top quark decay, Nuovo Cimento B 125 (2010) 983, http://dx.doi.org/10.1393/ncb/i2010-10896-0, arXiv:1010.2994.

[57] G.J. Feldman, R.D. Cousins, A unified approach to the classical statistical analysis of small signals, Phys. Rev. D 57 (1998) 3873, http://dx.doi.org/10.1103/PhysRevD.57.3873, arXiv:physics/9711021.

[58] L. Moneta, K. Belasco, K.S. Cranmer, A. Lazzaro, D. Piparo, G. Schott, W. Verkerke, M. Wolf, The RooStats Project, in: 13th International Workshop on Advanced Computing and Analysis Techniques in Physics Research, ACAT2010, SISSA, 2010, http://pos.sissa.it/archive/conferences/093/057/ACAT2010_057.pdf, arXiv:1009.1003, PoS(ACAT2010)057.

[59] N. Kidonakis, Next-to-next-to-leading-order collinear and soft gluon corrections for t-channel single top quark production, Phys. Rev. D 83 (2011) 091503, http://dx.doi.org/10.1103/PhysRevD.83.091503, arXiv:1103.2792.

CMS Collaboration

V. Khachatryan, A.M. Sirunyan, A. Tumasyan

Yerevan Physics Institute, Yerevan, Armenia

W. Adam, T. Bergauer, M. Dragicevic, J. Erö, C. Fabjan [1], M. Friedl, R. Frühwirth [1], V.M. Ghete, C. Hartl, N. Hörmann, J. Hrubec, M. Jeitler [1], W. Kiesenhofer, V. Knünz, M. Krammer [1], I. Krätschmer, D. Liko, I. Mikulec, D. Rabady [2], B. Rahbaran, H. Rohringer, R. Schöfbeck, J. Strauss, A. Taurok, W. Treberer-Treberspurg, W. Waltenberger, C.-E. Wulz [1]

Institut für Hochenergiephysik der OeAW, Wien, Austria

V. Mossolov, N. Shumeiko, J. Suarez Gonzalez

National Centre for Particle and High Energy Physics, Minsk, Belarus

S. Alderweireldt, M. Bansal, S. Bansal, T. Cornelis, E.A. De Wolf, X. Janssen, A. Knutsson, S. Luyckx, S. Ochesanu, B. Roland, R. Rougny, M. Van De Klundert, H. Van Haevermaet, P. Van Mechelen, N. Van Remortel, A. Van Spilbeeck

Universiteit Antwerpen, Antwerpen, Belgium

F. Blekman, S. Blyweert, J. D'Hondt, N. Daci, N. Heracleous, A. Kalogeropoulos, J. Keaveney, T.J. Kim, S. Lowette, M. Maes, A. Olbrechts, Q. Python, D. Strom, S. Tavernier, W. Van Doninck, P. Van Mulders, G.P. Van Onsem, I. Villella

Vrije Universiteit Brussel, Brussel, Belgium

C. Caillol, B. Clerbaux, G. De Lentdecker, L. Favart, A.P.R. Gay, A. Grebenyuk, A. Léonard, P.E. Marage, A. Mohammadi, L. Perniè, T. Reis, T. Seva, L. Thomas, C. Vander Velde, P. Vanlaer, J. Wang

Université Libre de Bruxelles, Bruxelles, Belgium

V. Adler, K. Beernaert, L. Benucci, A. Cimmino, S. Costantini, S. Crucy, S. Dildick, A. Fagot, G. Garcia, B. Klein, J. Mccartin, A.A. Ocampo Rios, D. Ryckbosch, S. Salva Diblen, M. Sigamani, N. Strobbe, F. Thyssen, M. Tytgat, E. Yazgan, N. Zaganidis

Ghent University, Ghent, Belgium

S. Basegmez, C. Beluffi [3], G. Bruno, R. Castello, A. Caudron, L. Ceard, G.G. Da Silveira, C. Delaere, T. du Pree, D. Favart, L. Forthomme, A. Giammanco [4], J. Hollar, P. Jez, M. Komm, V. Lemaitre, J. Liao, C. Nuttens, D. Pagano, A. Pin, K. Piotrzkowski, A. Popov [5], L. Quertenmont, M. Selvaggi, M. Vidal Marono, J.M. Vizan Garcia

Université Catholique de Louvain, Louvain-la-Neuve, Belgium

N. Beliy, T. Caebergs, E. Daubie, G.H. Hammad

Université de Mons, Mons, Belgium

G.A. Alves, M. Correa Martins Junior, T. Dos Reis Martins, M.E. Pol

Centro Brasileiro de Pesquisas Fisicas, Rio de Janeiro, Brazil

W.L. Aldá Júnior, W. Carvalho, J. Chinellato [6], A. Custódio, E.M. Da Costa, D. De Jesus Damiao, C. De Oliveira Martins, S. Fonseca De Souza, H. Malbouisson, M. Malek, D. Matos Figueiredo, L. Mundim, H. Nogima, W.L. Prado Da Silva, J. Santaolalla, A. Santoro, A. Sznajder, E.J. Tonelli Manganote [6], A. Vilela Pereira

Universidade do Estado do Rio de Janeiro, Rio de Janeiro, Brazil

C.A. Bernardes [b], F.A. Dias [a,7], T.R. Fernandez Perez Tomei [a], E.M. Gregores [b], P.G. Mercadante [b], S.F. Novaes [a], Sandra S. Padula [a]

[a] *Universidade Estadual Paulista, São Paulo, Brazil*
[b] *Universidade Federal do ABC, São Paulo, Brazil*

V. Genchev [2], P. Iaydjiev [2], A. Marinov, S. Piperov, M. Rodozov, G. Sultanov, M. Vutova

Institute for Nuclear Research and Nuclear Energy, Sofia, Bulgaria

A. Dimitrov, I. Glushkov, R. Hadjiiska, V. Kozhuharov, L. Litov, B. Pavlov, P. Petkov

University of Sofia, Sofia, Bulgaria

J.G. Bian, G.M. Chen, H.S. Chen, M. Chen, R. Du, C.H. Jiang, D. Liang, S. Liang, R. Plestina [8], J. Tao, X. Wang, Z. Wang

Institute of High Energy Physics, Beijing, China

C. Asawatangtrakuldee, Y. Ban, Y. Guo, Q. Li, W. Li, S. Liu, Y. Mao, S.J. Qian, D. Wang, L. Zhang, W. Zou

State Key Laboratory of Nuclear Physics and Technology, Peking University, Beijing, China

C. Avila, L.F. Chaparro Sierra, C. Florez, J.P. Gomez, B. Gomez Moreno, J.C. Sanabria

Universidad de Los Andes, Bogota, Colombia

N. Godinovic, D. Lelas, D. Polic, I. Puljak

Technical University of Split, Split, Croatia

Z. Antunovic, M. Kovac

University of Split, Split, Croatia

V. Brigljevic, K. Kadija, J. Luetic, D. Mekterovic, S. Morovic, L. Sudic

Institute Rudjer Boskovic, Zagreb, Croatia

A. Attikis, G. Mavromanolakis, J. Mousa, C. Nicolaou, F. Ptochos, P.A. Razis

University of Cyprus, Nicosia, Cyprus

M. Bodlak, M. Finger, M. Finger Jr.

Charles University, Prague, Czech Republic

Y. Assran [9], A. Ellithi Kamel [10], M.A. Mahmoud [11], A. Radi [12,13]

Academy of Scientific Research and Technology of the Arab Republic of Egypt, Egyptian Network of High Energy Physics, Cairo, Egypt

M. Kadastik, M. Murumaa, M. Raidal, A. Tiko

National Institute of Chemical Physics and Biophysics, Tallinn, Estonia

P. Eerola, G. Fedi, M. Voutilainen

Department of Physics, University of Helsinki, Helsinki, Finland

J. Härkönen, V. Karimäki, R. Kinnunen, M.J. Kortelainen, T. Lampén, K. Lassila-Perini, S. Lehti, T. Lindén, P. Luukka, T. Mäenpää, T. Peltola, E. Tuominen, J. Tuominiemi, E. Tuovinen, L. Wendland

Helsinki Institute of Physics, Helsinki, Finland

T. Tuuva

Lappeenranta University of Technology, Lappeenranta, Finland

M. Besancon, F. Couderc, M. Dejardin, D. Denegri, B. Fabbro, J.L. Faure, C. Favaro, F. Ferri, S. Ganjour, A. Givernaud, P. Gras, G. Hamel de Monchenault, P. Jarry, E. Locci, J. Malcles, A. Nayak, J. Rander, A. Rosowsky, M. Titov

DSM/IRFU, CEA/Saclay, Gif-sur-Yvette, France

S. Baffioni, F. Beaudette, P. Busson, C. Charlot, T. Dahms, M. Dalchenko, L. Dobrzynski, N. Filipovic, A. Florent, R. Granier de Cassagnac, L. Mastrolorenzo, P. Miné, C. Mironov, I.N. Naranjo, M. Nguyen, C. Ochando, P. Paganini, R. Salerno, J.b. Sauvan, Y. Sirois, C. Veelken, Y. Yilmaz, A. Zabi

Laboratoire Leprince-Ringuet, Ecole Polytechnique, IN2P3–CNRS, Palaiseau, France

J.-L. Agram [14], J. Andrea, A. Aubin, D. Bloch, J.-M. Brom, E.C. Chabert, C. Collard, E. Conte [14], J.-C. Fontaine [14], D. Gelé, U. Goerlach, C. Goetzmann, A.-C. Le Bihan, P. Van Hove

Institut Pluridisciplinaire Hubert Curien, Université de Strasbourg, Université de Haute Alsace Mulhouse, CNRS/IN2P3, Strasbourg, France

S. Gadrat

Centre de Calcul de l'Institut National de Physique Nucléaire et de Physique des Particules, CNRS/IN2P3, Villeurbanne, France

S. Beauceron, N. Beaupere, G. Boudoul, S. Brochet, C.A. Carrillo Montoya, J. Chasserat, R. Chierici, D. Contardo [2], P. Depasse, H. El Mamouni, J. Fan, J. Fay, S. Gascon, M. Gouzevitch, B. Ille, T. Kurca, M. Lethuillier, L. Mirabito, S. Perries, J.D. Ruiz Alvarez, D. Sabes, L. Sgandurra, V. Sordini, M. Vander Donckt, P. Verdier, S. Viret, H. Xiao

Université de Lyon, Université Claude Bernard Lyon 1, CNRS–IN2P3, Institut de Physique Nucléaire de Lyon, Villeurbanne, France

Z. Tsamalaidze [15]

Institute of High Energy Physics and Informatization, Tbilisi State University, Tbilisi, Georgia

C. Autermann, S. Beranek, M. Bontenackels, B. Calpas, M. Edelhoff, L. Feld, O. Hindrichs, K. Klein, A. Ostapchuk, A. Perieanu, F. Raupach, J. Sammet, S. Schael, D. Sprenger, H. Weber, B. Wittmer, V. Zhukov [5]

RWTH Aachen University, I. Physikalisches Institut, Aachen, Germany

M. Ata, J. Caudron, E. Dietz-Laursonn, D. Duchardt, M. Erdmann, R. Fischer, A. Güth, T. Hebbeker, C. Heidemann, K. Hoepfner, D. Klingebiel, S. Knutzen, P. Kreuzer, M. Merschmeyer, A. Meyer, M. Olschewski, K. Padeken, P. Papacz, H. Reithler, S.A. Schmitz, L. Sonnenschein, D. Teyssier, S. Thüer, M. Weber

RWTH Aachen University, III. Physikalisches Institut A, Aachen, Germany

V. Cherepanov, Y. Erdogan, G. Flügge, H. Geenen, M. Geisler, W. Haj Ahmad, F. Hoehle, B. Kargoll, T. Kress, Y. Kuessel, J. Lingemann [2], A. Nowack, I.M. Nugent, L. Perchalla, O. Pooth, A. Stahl

RWTH Aachen University, III. Physikalisches Institut B, Aachen, Germany

I. Asin, N. Bartosik, J. Behr, W. Behrenhoff, U. Behrens, A.J. Bell, M. Bergholz [16], A. Bethani, K. Borras, A. Burgmeier, A. Cakir, L. Calligaris, A. Campbell, S. Choudhury, F. Costanza, C. Diez Pardos, S. Dooling, T. Dorland, G. Eckerlin, D. Eckstein, T. Eichhorn, G. Flucke, J. Garay Garcia, A. Geiser, P. Gunnellini, J. Hauk, G. Hellwig, M. Hempel, D. Horton, H. Jung, M. Kasemann, P. Katsas, J. Kieseler, C. Kleinwort, D. Krücker, W. Lange, J. Leonard, K. Lipka, W. Lohmann [16], B. Lutz, R. Mankel, I. Marfin, I.-A. Melzer-Pellmann, A.B. Meyer, J. Mnich, A. Mussgiller, S. Naumann-Emme, O. Novgorodova, F. Nowak, E. Ntomari, H. Perrey, D. Pitzl, R. Placakyte, A. Raspereza, P.M. Ribeiro Cipriano, E. Ron, M.Ö. Sahin, J. Salfeld-Nebgen, P. Saxena, R. Schmidt [16], T. Schoerner-Sadenius, M. Schröder, A.D.R. Vargas Trevino, R. Walsh, C. Wissing

Deutsches Elektronen-Synchrotron, Hamburg, Germany

M. Aldaya Martin, V. Blobel, M. Centis Vignali, J. Erfle, E. Garutti, K. Goebel, M. Görner, M. Gosselink, J. Haller, R.S. Höing, H. Kirschenmann, R. Klanner, R. Kogler, J. Lange, T. Lapsien, T. Lenz, I. Marchesini, J. Ott, T. Peiffer, N. Pietsch, D. Rathjens, C. Sander, H. Schettler, P. Schleper, E. Schlieckau, A. Schmidt, M. Seidel, J. Sibille [17], V. Sola, H. Stadie, G. Steinbrück, D. Troendle, E. Usai, L. Vanelderen

University of Hamburg, Hamburg, Germany

C. Barth, C. Baus, J. Berger, C. Böser, E. Butz, T. Chwalek, W. De Boer, A. Descroix, A. Dierlamm, M. Feindt, M. Guthoff [2], F. Hartmann [2], T. Hauth [2], U. Husemann, I. Katkov [5], A. Kornmayer [2], E. Kuznetsova, P. Lobelle Pardo, M.U. Mozer, Th. Müller, A. Nürnberg, G. Quast, K. Rabbertz, F. Ratnikov, S. Röcker, H.J. Simonis, F.M. Stober, R. Ulrich, J. Wagner-Kuhr, S. Wayand, T. Weiler

Institut für Experimentelle Kernphysik, Karlsruhe, Germany

G. Anagnostou, G. Daskalakis, T. Geralis, V.A. Giakoumopoulou, A. Kyriakis, D. Loukas, A. Markou, C. Markou, A. Psallidas, I. Topsis-Giotis

Institute of Nuclear and Particle Physics (INPP), NCSR Demokritos, Aghia Paraskevi, Greece

L. Gouskos, A. Panagiotou, N. Saoulidou, E. Stiliaris

University of Athens, Athens, Greece

X. Aslanoglou, I. Evangelou [2], G. Flouris, C. Foudas [2], P. Kokkas, N. Manthos, I. Papadopoulos, E. Paradas

University of Ioánnina, Ioánnina, Greece

G. Bencze [2], C. Hajdu, P. Hidas, D. Horvath [18], F. Sikler, V. Veszpremi, G. Vesztergombi [19], A.J. Zsigmond

Wigner Research Centre for Physics, Budapest, Hungary

N. Beni, S. Czellar, J. Karancsi [20], J. Molnar, J. Palinkas, Z. Szillasi

Institute of Nuclear Research ATOMKI, Debrecen, Hungary

P. Raics, Z.L. Trocsanyi, B. Ujvari

University of Debrecen, Debrecen, Hungary

S.K. Swain

National Institute of Science Education and Research, Bhubaneswar, India

S.B. Beri, V. Bhatnagar, N. Dhingra, R. Gupta, A.K. Kalsi, M. Kaur, M. Mittal, N. Nishu, J.B. Singh

Panjab University, Chandigarh, India

Ashok Kumar, Arun Kumar, S. Ahuja, A. Bhardwaj, B.C. Choudhary, A. Kumar, S. Malhotra, M. Naimuddin, K. Ranjan, V. Sharma

University of Delhi, Delhi, India

S. Banerjee, S. Bhattacharya, K. Chatterjee, S. Dutta, B. Gomber, Sa. Jain, Sh. Jain, R. Khurana, A. Modak, S. Mukherjee, D. Roy, S. Sarkar, M. Sharan

Saha Institute of Nuclear Physics, Kolkata, India

A. Abdulsalam, D. Dutta, S. Kailas, V. Kumar, A.K. Mohanty [2], L.M. Pant, P. Shukla, A. Topkar

Bhabha Atomic Research Centre, Mumbai, India

T. Aziz, R.M. Chatterjee, S. Ganguly, S. Ghosh, M. Guchait [21], A. Gurtu [22], G. Kole, S. Kumar, M. Maity [23], G. Majumder, K. Mazumdar, G.B. Mohanty, B. Parida, K. Sudhakar, N. Wickramage [24]

Tata Institute of Fundamental Research – EHEP, Mumbai, India

S. Banerjee, R.K. Dewanjee, S. Dugad

Tata Institute of Fundamental Research – HECR, Mumbai, India

H. Bakhshiansohi, H. Behnamian, S.M. Etesami [25], A. Fahim [26], A. Jafari, M. Khakzad, M. Mohammadi Najafabadi, M. Naseri, S. Paktinat Mehdiabadi, B. Safarzadeh [27], M. Zeinali

Institute for Research in Fundamental Sciences (IPM), Tehran, Iran

M. Felcini, M. Grunewald

University College Dublin, Dublin, Ireland

M. Abbrescia [a,b], L. Barbone [a,b], C. Calabria [a,b], S.S. Chhibra [a,b], A. Colaleo [a], D. Creanza [a,c], N. De Filippis [a,c], M. De Palma [a,b], L. Fiore [a], G. Iaselli [a,c], G. Maggi [a,c], M. Maggi [a], S. My [a,c], S. Nuzzo [a,b], N. Pacifico [a], A. Pompili [a,b], G. Pugliese [a,c], R. Radogna [a,b], G. Selvaggi [a,b], L. Silvestris [a], G. Singh [a,b], R. Venditti [a,b], P. Verwilligen [a], G. Zito [a]

[a] *INFN Sezione di Bari, Bari, Italy*
[b] *Università di Bari, Bari, Italy*
[c] *Politecnico di Bari, Bari, Italy*

G. Abbiendi [a], A.C. Benvenuti [a], D. Bonacorsi [a,b], S. Braibant-Giacomelli [a,b], L. Brigliadori [a,b], R. Campanini [a,b], P. Capiluppi [a,b], A. Castro [a,b], F.R. Cavallo [a], G. Codispoti [a,b], M. Cuffiani [a,b], G.M. Dallavalle [a], F. Fabbri [a], A. Fanfani [a,b], D. Fasanella [a,b], P. Giacomelli [a], C. Grandi [a], L. Guiducci [a,b], S. Marcellini [a], G. Masetti [a], A. Montanari [a], F.L. Navarria [a,b], A. Perrotta [a], F. Primavera [a,b], A.M. Rossi [a,b], T. Rovelli [a,b], G.P. Siroli [a,b], N. Tosi [a,b], R. Travaglini [a,b]

[a] *INFN Sezione di Bologna, Bologna, Italy*
[b] *Università di Bologna, Bologna, Italy*

S. Albergo [a,b], G. Cappello [a], M. Chiorboli [a,b], S. Costa [a,b], F. Giordano [a,2], R. Potenza [a,b], A. Tricomi [a,b], C. Tuve [a,b]

[a] *INFN Sezione di Catania, Catania, Italy*
[b] *Università di Catania, Catania, Italy*
[c] *CSFNSM, Catania, Italy*

G. Barbagli [a], V. Ciulli [a,b], C. Civinini [a], R. D'Alessandro [a,b], E. Focardi [a,b], E. Gallo [a], S. Gonzi [a,b], V. Gori [a,b], P. Lenzi [a,b], M. Meschini [a], S. Paoletti [a], G. Sguazzoni [a], A. Tropiano [a,b]

[a] *INFN Sezione di Firenze, Firenze, Italy*
[b] *Università di Firenze, Firenze, Italy*

L. Benussi, S. Bianco, F. Fabbri, D. Piccolo

INFN Laboratori Nazionali di Frascati, Frascati, Italy

F. Ferro [a], M. Lo Vetere [a,b], E. Robutti [a], S. Tosi [a,b]

[a] *INFN Sezione di Genova, Genova, Italy*
[b] *Università di Genova, Genova, Italy*

M.E. Dinardo [a,b], S. Fiorendi [a,b,2], S. Gennai [a], R. Gerosa, A. Ghezzi [a,b], P. Govoni [a,b], M.T. Lucchini [a,b,2], S. Malvezzi [a], R.A. Manzoni [a,b,2], A. Martelli [a,b,2], B. Marzocchi, D. Menasce [a], L. Moroni [a], M. Paganoni [a,b], D. Pedrini [a], S. Ragazzi [a,b], N. Redaelli [a], T. Tabarelli de Fatis [a,b]

[a] *INFN Sezione di Milano-Bicocca, Milano, Italy*
[b] *Università di Milano-Bicocca, Milano, Italy*

S. Buontempo [a], N. Cavallo [a,c], S. Di Guida [a,d], F. Fabozzi [a,c], A.O.M. Iorio [a,b], L. Lista [a], S. Meola [a,d,2], M. Merola [a], P. Paolucci [a,2]

[a] *INFN Sezione di Napoli, Napoli, Italy*
[b] *Università di Napoli 'Federico II', Napoli, Italy*
[c] *Università della Basilicata (Potenza), Napoli, Italy*
[d] *Università G. Marconi (Roma), Napoli, Italy*

P. Azzi [a], N. Bacchetta [a], D. Bisello [a,b], A. Branca [a,b], R. Carlin [a,b], P. Checchia [a], T. Dorigo [a], U. Dosselli [a], M. Galanti [a,b], F. Gasparini [a,b], U. Gasparini [a,b], F. Gonella [a], A. Gozzelino [a], K. Kanishchev [a,c], S. Lacaprara [a], M. Margoni [a,b], A.T. Meneguzzo [a,b], J. Pazzini [a,b], N. Pozzobon [a,b], P. Ronchese [a,b], F. Simonetto [a,b], E. Torassa [a], M. Tosi [a,b], P. Zotto [a,b], A. Zucchetta [a,b], G. Zumerle [a,b]

[a] *INFN Sezione di Padova, Padova, Italy*
[b] *Università di Padova, Padova, Italy*
[c] *Università di Trento (Trento), Padova, Italy*

M. Gabusi [a,b], S.P. Ratti [a,b], C. Riccardi [a,b], P. Salvini [a], P. Vitulo [a,b]

[a] *INFN Sezione di Pavia, Pavia, Italy*
[b] *Università di Pavia, Pavia, Italy*

M. Biasini [a,b], G.M. Bilei [a], L. Fanò [a,b], P. Lariccia [a,b], G. Mantovani [a,b], M. Menichelli [a], F. Romeo [a,b], A. Saha [a], A. Santocchia [a,b], A. Spiezia [a,b]

[a] *INFN Sezione di Perugia, Perugia, Italy*
[b] *Università di Perugia, Perugia, Italy*

K. Androsov [a,28], P. Azzurri [a], G. Bagliesi [a], J. Bernardini [a], T. Boccali [a], G. Broccolo [a,c], R. Castaldi [a], M.A. Ciocci [a,28], R. Dell'Orso [a], S. Donato [a,c], F. Fiori [a,c], L. Foà [a,c], A. Giassi [a], M.T. Grippo [a,28], F. Ligabue [a,c], T. Lomtadze [a], L. Martini [a,b], A. Messineo [a,b], C.S. Moon [a,29], F. Palla [a,2], A. Rizzi [a,b], A. Savoy-Navarro [a,30], A.T. Serban [a], P. Spagnolo [a], P. Squillacioti [a,28], R. Tenchini [a], G. Tonelli [a,b], A. Venturi [a], P.G. Verdini [a], C. Vernieri [a,c]

[a] *INFN Sezione di Pisa, Pisa, Italy*
[b] *Università di Pisa, Pisa, Italy*
[c] *Scuola Normale Superiore di Pisa, Pisa, Italy*

L. Barone [a,b], F. Cavallari [a], D. Del Re [a,b], M. Diemoz [a], M. Grassi [a,b], C. Jorda [a], E. Longo [a,b], F. Margaroli [a,b], P. Meridiani [a], F. Micheli [a,b], S. Nourbakhsh [a,b], G. Organtini [a,b], R. Paramatti [a], S. Rahatlou [a,b], C. Rovelli [a], F. Santanastasio [a,b], L. Soffi [a,b], P. Traczyk [a,b]

[a] *INFN Sezione di Roma, Roma, Italy*
[b] *Università di Roma, Roma, Italy*

N. Amapane [a,b], R. Arcidiacono [a,c], S. Argiro [a,b], M. Arneodo [a,c], R. Bellan [a,b], C. Biino [a], N. Cartiglia [a], S. Casasso [a,b], M. Costa [a,b], A. Degano [a,b], N. Demaria [a], L. Finco [a,b], C. Mariotti [a], S. Maselli [a], E. Migliore [a,b], V. Monaco [a,b], M. Musich [a], M.M. Obertino [a,c], G. Ortona [a,b], L. Pacher [a,b], N. Pastrone [a], M. Pelliccioni [a,2], G.L. Pinna Angioni [a,b], A. Potenza [a,b], A. Romero [a,b], M. Ruspa [a,c], R. Sacchi [a,b], A. Solano [a,b], A. Staiano [a], U. Tamponi [a]

[a] INFN Sezione di Torino, Torino, Italy
[b] Università di Torino, Torino, Italy
[c] Università del Piemonte Orientale (Novara), Torino, Italy

S. Belforte [a], V. Candelise [a,b], M. Casarsa [a], F. Cossutti [a], G. Della Ricca [a,b], B. Gobbo [a], C. La Licata [a,b], M. Marone [a,b], D. Montanino [a,b], A. Schizzi [a,b], T. Umer [a,b], A. Zanetti [a]

[a] INFN Sezione di Trieste, Trieste, Italy
[b] Università di Trieste, Trieste, Italy

S. Chang, S.K. Nam

Kangwon National University, Chunchon, Republic of Korea

D.H. Kim, G.N. Kim, M.S. Kim, D.J. Kong, S. Lee, Y.D. Oh, H. Park, A. Sakharov, D.C. Son

Kyungpook National University, Daegu, Republic of Korea

J.Y. Kim, S. Song

Chonnam National University, Institute for Universe and Elementary Particles, Kwangju, Republic of Korea

S. Choi, D. Gyun, B. Hong, M. Jo, H. Kim, Y. Kim, B. Lee, K.S. Lee, S.K. Park, Y. Roh

Korea University, Seoul, Republic of Korea

M. Choi, J.H. Kim, I.C. Park, S. Park, G. Ryu, M.S. Ryu

University of Seoul, Seoul, Republic of Korea

Y. Choi, Y.K. Choi, J. Goh, E. Kwon, J. Lee, H. Seo, I. Yu

Sungkyunkwan University, Suwon, Republic of Korea

A. Juodagalvis

Vilnius University, Vilnius, Lithuania

J.R. Komaragiri

National Centre for Particle Physics, Universiti Malaya, Kuala Lumpur, Malaysia

H. Castilla-Valdez, E. De La Cruz-Burelo, I. Heredia-de La Cruz [31], R. Lopez-Fernandez, J. Martínez-Ortega, A. Sanchez-Hernandez, L.M. Villasenor-Cendejas

Centro de Investigacion y de Estudios Avanzados del IPN, Mexico City, Mexico

S. Carrillo Moreno, F. Vazquez Valencia

Universidad Iberoamericana, Mexico City, Mexico

I. Pedraza, H.A. Salazar Ibarguen

Benemerita Universidad Autonoma de Puebla, Puebla, Mexico

E. Casimiro Linares, A. Morelos Pineda

Universidad Autónoma de San Luis Potosí, San Luis Potosí, Mexico

D. Krofcheck

University of Auckland, Auckland, New Zealand

P.H. Butler, S. Reucroft

University of Canterbury, Christchurch, New Zealand

A. Ahmad, M. Ahmad, Q. Hassan, H.R. Hoorani, S. Khalid, W.A. Khan, T. Khurshid, M.A. Shah, M. Shoaib

National Centre for Physics, Quaid-I-Azam University, Islamabad, Pakistan

H. Bialkowska, M. Bluj [32], B. Boimska, T. Frueboes, M. Górski, M. Kazana, K. Nawrocki,
K. Romanowska-Rybinska, M. Szleper, P. Zalewski

National Centre for Nuclear Research, Swierk, Poland

G. Brona, K. Bunkowski, M. Cwiok, W. Dominik, K. Doroba, A. Kalinowski, M. Konecki, J. Krolikowski,
M. Misiura, M. Olszewski, W. Wolszczak

Institute of Experimental Physics, Faculty of Physics, University of Warsaw, Warsaw, Poland

P. Bargassa, C. Beirão Da Cruz E Silva, P. Faccioli, P.G. Ferreira Parracho, M. Gallinaro, F. Nguyen,
J. Rodrigues Antunes, J. Seixas, J. Varela, P. Vischia

Laboratório de Instrumentação e Física Experimental de Partículas, Lisboa, Portugal

S. Afanasiev, P. Bunin, M. Gavrilenko, I. Golutvin, I. Gorbunov, A. Kamenev, V. Karjavin, V. Konoplyanikov,
A. Lanev, A. Malakhov, V. Matveev [33], P. Moisenz, V. Palichik, V. Perelygin, S. Shmatov, N. Skatchkov,
V. Smirnov, A. Zarubin

Joint Institute for Nuclear Research, Dubna, Russia

V. Golovtsov, Y. Ivanov, V. Kim [34], P. Levchenko, V. Murzin, V. Oreshkin, I. Smirnov, V. Sulimov, L. Uvarov,
S. Vavilov, A. Vorobyev, An. Vorobyev

Petersburg Nuclear Physics Institute, Gatchina (St. Petersburg), Russia

Yu. Andreev, A. Dermenev, S. Gninenko, N. Golubev, M. Kirsanov, N. Krasnikov, A. Pashenkov, D. Tlisov,
A. Toropin

Institute for Nuclear Research, Moscow, Russia

V. Epshteyn, V. Gavrilov, N. Lychkovskaya, V. Popov, G. Safronov, S. Semenov, A. Spiridonov, V. Stolin,
E. Vlasov, A. Zhokin

Institute for Theoretical and Experimental Physics, Moscow, Russia

V. Andreev, M. Azarkin, I. Dremin, M. Kirakosyan, A. Leonidov, G. Mesyats, S.V. Rusakov, A. Vinogradov

P.N. Lebedev Physical Institute, Moscow, Russia

A. Belyaev, E. Boos, M. Dubinin [7], L. Dudko, A. Ershov, A. Gribushin, V. Klyukhin, O. Kodolova, I. Lokhtin,
S. Obraztsov, S. Petrushanko, V. Savrin, A. Snigirev

Skobeltsyn Institute of Nuclear Physics, Lomonosov Moscow State University, Moscow, Russia

I. Azhgirey, I. Bayshev, S. Bitioukov, V. Kachanov, A. Kalinin, D. Konstantinov, V. Krychkine, V. Petrov,
R. Ryutin, A. Sobol, L. Tourtchanovitch, S. Troshin, N. Tyurin, A. Uzunian, A. Volkov

State Research Center of Russian Federation, Institute for High Energy Physics, Protvino, Russia

P. Adzic [35], M. Djordjevic, M. Ekmedzic, J. Milosevic

University of Belgrade, Faculty of Physics and Vinca Institute of Nuclear Sciences, Belgrade, Serbia

J. Alcaraz Maestre, C. Battilana, E. Calvo, M. Cerrada, M. Chamizo Llatas [2], N. Colino, B. De La Cruz,
A. Delgado Peris, D. Domínguez Vázquez, A. Escalante Del Valle, C. Fernandez Bedoya,
J.P. Fernández Ramos, J. Flix, M.C. Fouz, P. Garcia-Abia, O. Gonzalez Lopez, S. Goy Lopez, J.M. Hernandez,
M.I. Josa, G. Merino, E. Navarro De Martino, A. Pérez-Calero Yzquierdo, J. Puerta Pelayo,
A. Quintario Olmeda, I. Redondo, L. Romero, M.S. Soares

Centro de Investigaciones Energéticas Medioambientales y Tecnológicas (CIEMAT), Madrid, Spain

C. Albajar, J.F. de Trocóniz, M. Missiroli

Universidad Autónoma de Madrid, Madrid, Spain

H. Brun, J. Cuevas, J. Fernandez Menendez, S. Folgueras, I. Gonzalez Caballero, L. Lloret Iglesias

Universidad de Oviedo, Oviedo, Spain

J.A. Brochero Cifuentes, I.J. Cabrillo, A. Calderon, J. Duarte Campderros, M. Fernandez, G. Gomez,
J. Gonzalez Sanchez, A. Graziano, A. Lopez Virto, J. Marco, R. Marco, C. Martinez Rivero, F. Matorras,
F.J. Munoz Sanchez, J. Piedra Gomez, T. Rodrigo, A.Y. Rodríguez-Marrero, A. Ruiz-Jimeno, L. Scodellaro,
I. Vila, R. Vilar Cortabitarte

Instituto de Física de Cantabria (IFCA), CSIC–Universidad de Cantabria, Santander, Spain

D. Abbaneo, E. Auffray, G. Auzinger, M. Bachtis, P. Baillon, A.H. Ball, D. Barney, A. Benaglia, J. Bendavid,
L. Benhabib, J.F. Benitez, C. Bernet [8], G. Bianchi, P. Bloch, A. Bocci, A. Bonato, O. Bondu, C. Botta,
H. Breuker, T. Camporesi, G. Cerminara, T. Christiansen, S. Colafranceschi [36], M. D'Alfonso, D. d'Enterria,
A. Dabrowski, A. David, F. De Guio, A. De Roeck, S. De Visscher, M. Dobson, N. Dupont-Sagorin,
A. Elliott-Peisert, J. Eugster, G. Franzoni, W. Funk, M. Giffels, D. Gigi, K. Gill, D. Giordano, M. Girone,
F. Glege, R. Guida, J. Hammer, M. Hansen, P. Harris, J. Hegeman, V. Innocente, P. Janot, E. Karavakis,
K. Kousouris, K. Krajczar, P. Lecoq, C. Lourenço, N. Magini, L. Malgeri, M. Mannelli, L. Masetti, F. Meijers,
S. Mersi, E. Meschi, F. Moortgat, M. Mulders, P. Musella, L. Orsini, L. Pape, E. Perez, L. Perrozzi, A. Petrilli,
G. Petrucciani, A. Pfeiffer, M. Pierini, M. Pimiä, D. Piparo, M. Plagge, A. Racz, G. Rolandi [37], M. Rovere,
H. Sakulin, C. Schäfer, C. Schwick, S. Sekmen, A. Sharma, P. Siegrist, P. Silva, M. Simon, P. Sphicas [38],
D. Spiga, J. Steggemann, B. Stieger, M. Stoye, D. Treille, A. Tsirou, G.I. Veres [19], J.R. Vlimant, H.K. Wöhri,
W.D. Zeuner

CERN, European Organization for Nuclear Research, Geneva, Switzerland

W. Bertl, K. Deiters, W. Erdmann, R. Horisberger, Q. Ingram, H.C. Kaestli, S. König, D. Kotlinski,
U. Langenegger, D. Renker, T. Rohe

Paul Scherrer Institut, Villigen, Switzerland

F. Bachmair, L. Bäni, L. Bianchini, P. Bortignon, M.A. Buchmann, B. Casal, N. Chanon, A. Deisher,
G. Dissertori, M. Dittmar, M. Donegà, M. Dünser, P. Eller, C. Grab, D. Hits, W. Lustermann, B. Mangano,
A.C. Marini, P. Martinez Ruiz del Arbol, D. Meister, N. Mohr, C. Nägeli [39], P. Nef, F. Nessi-Tedaldi,
F. Pandolfi, F. Pauss, M. Peruzzi, M. Quittnat, L. Rebane, F.J. Ronga, M. Rossini, A. Starodumov [40],
M. Takahashi, K. Theofilatos, R. Wallny, H.A. Weber

Institute for Particle Physics, ETH Zurich, Zurich, Switzerland

C. Amsler [41], M.F. Canelli, V. Chiochia, A. De Cosa, A. Hinzmann, T. Hreus, M. Ivova Rikova, B. Kilminster,
B. Millan Mejias, J. Ngadiuba, P. Robmann, H. Snoek, S. Taroni, M. Verzetti, Y. Yang

Universität Zürich, Zurich, Switzerland

M. Cardaci, K.H. Chen, C. Ferro, C.M. Kuo, W. Lin, Y.J. Lu, R. Volpe, S.S. Yu

National Central University, Chung-Li, Taiwan

P. Chang, Y.H. Chang, Y.W. Chang, Y. Chao, K.F. Chen, P.H. Chen, C. Dietz, U. Grundler, W.-S. Hou, K.Y. Kao, Y.J. Lei, Y.F. Liu, R.-S. Lu, D. Majumder, E. Petrakou, X. Shi, Y.M. Tzeng, R. Wilken

National Taiwan University (NTU), Taipei, Taiwan

B. Asavapibhop, N. Srimanobhas, N. Suwonjandee

Chulalongkorn University, Bangkok, Thailand

A. Adiguzel, M.N. Bakirci [42], S. Cerci [43], C. Dozen, I. Dumanoglu, E. Eskut, S. Girgis, G. Gokbulut, E. Gurpinar, I. Hos, E.E. Kangal, A. Kayis Topaksu, G. Onengut [44], K. Ozdemir, S. Ozturk [42], A. Polatoz, K. Sogut [45], D. Sunar Cerci [43], B. Tali [43], H. Topakli [42], M. Vergili

Cukurova University, Adana, Turkey

I.V. Akin, B. Bilin, S. Bilmis, H. Gamsizkan, G. Karapinar [46], K. Ocalan, U.E. Surat, M. Yalvac, M. Zeyrek

Middle East Technical University, Physics Department, Ankara, Turkey

E. Gülmez, B. Isildak [47], M. Kaya [48], O. Kaya [48]

Bogazici University, Istanbul, Turkey

H. Bahtiyar [49], E. Barlas, K. Cankocak, F.I. Vardarlı, M. Yücel

Istanbul Technical University, Istanbul, Turkey

L. Levchuk, P. Sorokin

National Scientific Center, Kharkov Institute of Physics and Technology, Kharkov, Ukraine

J.J. Brooke, E. Clement, D. Cussans, H. Flacher, R. Frazier, J. Goldstein, M. Grimes, G.P. Heath, H.F. Heath, J. Jacob, L. Kreczko, C. Lucas, Z. Meng, D.M. Newbold [50], S. Paramesvaran, A. Poll, S. Senkin, V.J. Smith, T. Williams

University of Bristol, Bristol, United Kingdom

K.W. Bell, A. Belyaev [51], C. Brew, R.M. Brown, D.J.A. Cockerill, J.A. Coughlan, K. Harder, S. Harper, E. Olaiya, D. Petyt, C.H. Shepherd-Themistocleous, A. Thea, I.R. Tomalin, W.J. Womersley, S.D. Worm

Rutherford Appleton Laboratory, Didcot, United Kingdom

M. Baber, R. Bainbridge, O. Buchmuller, D. Burton, D. Colling, N. Cripps, M. Cutajar, P. Dauncey, G. Davies, M. Della Negra, P. Dunne, W. Ferguson, J. Fulcher, D. Futyan, A. Gilbert, A. Guneratne Bryer, G. Hall, Z. Hatherell, G. Iles, M. Jarvis, G. Karapostoli, M. Kenzie, R. Lane, R. Lucas [50], L. Lyons, A.-M. Magnan, S. Malik, J. Marrouche, B. Mathias, R. Nandi, J. Nash, A. Nikitenko [40], J. Pela, M. Pesaresi, K. Petridis, D.M. Raymond, S. Rogerson, A. Rose, C. Seez, P. Sharp [†], A. Sparrow, A. Tapper, M. Vazquez Acosta, T. Virdee, S. Wakefield

Imperial College, London, United Kingdom

J.E. Cole, P.R. Hobson, A. Khan, P. Kyberd, D. Leggat, D. Leslie, W. Martin, I.D. Reid, P. Symonds, L. Teodorescu, M. Turner

Brunel University, Uxbridge, United Kingdom

J. Dittmann, K. Hatakeyama, A. Kasmi, H. Liu, T. Scarborough

Baylor University, Waco, USA

O. Charaf, S.I. Cooper, C. Henderson, P. Rumerio

The University of Alabama, Tuscaloosa, USA

A. Avetisyan, T. Bose, C. Fantasia, A. Heister, P. Lawson, C. Richardson, J. Rohlf, D. Sperka, J. St. John,
L. Sulak

Boston University, Boston, USA

J. Alimena, S. Bhattacharya, G. Christopher, D. Cutts, Z. Demiragli, A. Ferapontov, A. Garabedian,
U. Heintz, S. Jabeen, G. Kukartsev, E. Laird, G. Landsberg, M. Luk, M. Narain, M. Segala, T. Sinthuprasith,
T. Speer, J. Swanson

Brown University, Providence, USA

R. Breedon, G. Breto, M. Calderon De La Barca Sanchez, S. Chauhan, M. Chertok, J. Conway, R. Conway,
P.T. Cox, R. Erbacher, M. Gardner, W. Ko, A. Kopecky, R. Lander, T. Miceli, M. Mulhearn, D. Pellett, J. Pilot,
F. Ricci-Tam, B. Rutherford, M. Searle, S. Shalhout, J. Smith, M. Squires, M. Tripathi, S. Wilbur, R. Yohay

University of California, Davis, Davis, USA

R. Cousins, P. Everaerts, C. Farrell, J. Hauser, M. Ignatenko, G. Rakness, E. Takasugi, V. Valuev, M. Weber

University of California, Los Angeles, USA

J. Babb, R. Clare, J. Ellison, J.W. Gary, G. Hanson, J. Heilman, P. Jandir, F. Lacroix, H. Liu, O.R. Long,
A. Luthra, M. Malberti, H. Nguyen, A. Shrinivas, J. Sturdy, S. Sumowidagdo, S. Wimpenny

University of California, Riverside, Riverside, USA

W. Andrews, J.G. Branson, G.B. Cerati, S. Cittolin, R.T. D'Agnolo, D. Evans, A. Holzner, R. Kelley,
M. Lebourgeois, J. Letts, I. Macneill, S. Padhi, C. Palmer, M. Pieri, M. Sani, V. Sharma, S. Simon, E. Sudano,
M. Tadel, Y. Tu, A. Vartak, F. Würthwein, A. Yagil, J. Yoo

University of California, San Diego, La Jolla, USA

D. Barge, J. Bradmiller-Feld, C. Campagnari, T. Danielson, A. Dishaw, K. Flowers, M. Franco Sevilla,
P. Geffert, C. George, F. Golf, J. Incandela, C. Justus, N. Mccoll, J. Richman, D. Stuart, W. To, C. West

University of California, Santa Barbara, Santa Barbara, USA

A. Apresyan, A. Bornheim, J. Bunn, Y. Chen, E. Di Marco, J. Duarte, A. Mott, H.B. Newman, C. Pena,
C. Rogan, M. Spiropulu, V. Timciuc, R. Wilkinson, S. Xie, R.Y. Zhu

California Institute of Technology, Pasadena, USA

V. Azzolini, A. Calamba, R. Carroll, T. Ferguson, Y. Iiyama, M. Paulini, J. Russ, H. Vogel, I. Vorobiev

Carnegie Mellon University, Pittsburgh, USA

J.P. Cumalat, B.R. Drell, W.T. Ford, A. Gaz, E. Luiggi Lopez, U. Nauenberg, J.G. Smith, K. Stenson,
K.A. Ulmer, S.R. Wagner

University of Colorado at Boulder, Boulder, USA

J. Alexander, A. Chatterjee, J. Chu, N. Eggert, W. Hopkins, A. Khukhunaishvili, B. Kreis, N. Mirman,
G. Nicolas Kaufman, J.R. Patterson, A. Ryd, E. Salvati, L. Skinnari, W. Sun, W.D. Teo, J. Thom, J. Thompson,
J. Tucker, Y. Weng, L. Winstrom, P. Wittich

Cornell University, Ithaca, USA

D. Winn

Fairfield University, Fairfield, USA

S. Abdullin, M. Albrow, J. Anderson, G. Apollinari, L.A.T. Bauerdick, A. Beretvas, J. Berryhill, P.C. Bhat,
K. Burkett, J.N. Butler, H.W.K. Cheung, F. Chlebana, S. Cihangir, V.D. Elvira, I. Fisk, J. Freeman,

E. Gottschalk, L. Gray, D. Green, S. Grünendahl, O. Gutsche, J. Hanlon, D. Hare, R.M. Harris, J. Hirschauer, B. Hooberman, S. Jindariani, M. Johnson, U. Joshi, K. Kaadze, B. Klima, S. Kwan, J. Linacre, D. Lincoln, R. Lipton, T. Liu, J. Lykken, K. Maeshima, J.M. Marraffino, V.I. Martinez Outschoorn, S. Maruyama, D. Mason, P. McBride, K. Mishra, S. Mrenna, Y. Musienko [33], S. Nahn, C. Newman-Holmes, V. O'Dell, O. Prokofyev, E. Sexton-Kennedy, S. Sharma, A. Soha, W.J. Spalding, L. Spiegel, L. Taylor, S. Tkaczyk, N.V. Tran, L. Uplegger, E.W. Vaandering, R. Vidal, J. Whitmore, F. Yang

Fermi National Accelerator Laboratory, Batavia, USA

D. Acosta, P. Avery, D. Bourilkov, T. Cheng, S. Das, M. De Gruttola, G.P. Di Giovanni, D. Dobur, R.D. Field, M. Fisher, I.K. Furic, J. Hugon, J. Konigsberg, A. Korytov, A. Kropivnitskaya, T. Kypreos, J.F. Low, K. Matchev, P. Milenovic [52], G. Mitselmakher, L. Muniz, A. Rinkevicius, L. Shchutska, N. Skhirtladze, M. Snowball, J. Yelton, M. Zakaria

University of Florida, Gainesville, USA

V. Gaultney, S. Hewamanage, S. Linn, P. Markowitz, G. Martinez, J.L. Rodriguez

Florida International University, Miami, USA

T. Adams, A. Askew, J. Bochenek, B. Diamond, J. Haas, S. Hagopian, V. Hagopian, K.F. Johnson, H. Prosper, V. Veeraraghavan, M. Weinberg

Florida State University, Tallahassee, USA

M.M. Baarmand, M. Hohlmann, H. Kalakhety, F. Yumiceva

Florida Institute of Technology, Melbourne, USA

M.R. Adams, L. Apanasevich, V.E. Bazterra, R.R. Betts, I. Bucinskaite, R. Cavanaugh, O. Evdokimov, L. Gauthier, C.E. Gerber, D.J. Hofman, S. Khalatyan, P. Kurt, D.H. Moon, C. O'Brien, C. Silkworth, P. Turner, N. Varelas

University of Illinois at Chicago (UIC), Chicago, USA

E.A. Albayrak [49], B. Bilki [53], W. Clarida, K. Dilsiz, F. Duru, M. Haytmyradov, J.-P. Merlo, H. Mermerkaya [54], A. Mestvirishvili, A. Moeller, J. Nachtman, H. Ogul, Y. Onel, F. Ozok [49], A. Penzo, R. Rahmat, S. Sen, P. Tan, E. Tiras, J. Wetzel, T. Yetkin [55], K. Yi

The University of Iowa, Iowa City, USA

B.A. Barnett, B. Blumenfeld, D. Fehling, A.V. Gritsan, P. Maksimovic, C. Martin, M. Swartz

Johns Hopkins University, Baltimore, USA

P. Baringer, A. Bean, G. Benelli, J. Gray, R.P. Kenny III, M. Murray, D. Noonan, S. Sanders, J. Sekaric, R. Stringer, Q. Wang, J.S. Wood

The University of Kansas, Lawrence, USA

A.F. Barfuss, I. Chakaberia, A. Ivanov, S. Khalil, M. Makouski, Y. Maravin, L.K. Saini, S. Shrestha, I. Svintradze

Kansas State University, Manhattan, USA

J. Gronberg, D. Lange, F. Rebassoo, D. Wright

Lawrence Livermore National Laboratory, Livermore, USA

A. Baden, B. Calvert, S.C. Eno, J.A. Gomez, N.J. Hadley, R.G. Kellogg, T. Kolberg, Y. Lu, M. Marionneau, A.C. Mignerey, K. Pedro, A. Skuja, M.B. Tonjes, S.C. Tonwar

University of Maryland, College Park, USA

A. Apyan, R. Barbieri, G. Bauer, W. Busza, I.A. Cali, M. Chan, L. Di Matteo, V. Dutta, G. Gomez Ceballos, M. Goncharov, D. Gulhan, M. Klute, Y.S. Lai, Y.-J. Lee, A. Levin, P.D. Luckey, T. Ma, C. Paus, D. Ralph, C. Roland, G. Roland, G.S.F. Stephans, F. Stöckli, K. Sumorok, D. Velicanu, J. Veverka, B. Wyslouch, M. Yang, M. Zanetti, V. Zhukova

Massachusetts Institute of Technology, Cambridge, USA

B. Dahmes, A. De Benedetti, A. Gude, S.C. Kao, K. Klapoetke, Y. Kubota, J. Mans, N. Pastika, R. Rusack, A. Singovsky, N. Tambe, J. Turkewitz

University of Minnesota, Minneapolis, USA

J.G. Acosta, S. Oliveros

University of Mississippi, Oxford, USA

E. Avdeeva, K. Bloom, S. Bose, D.R. Claes, A. Dominguez, R. Gonzalez Suarez, J. Keller, D. Knowlton, I. Kravchenko, J. Lazo-Flores, S. Malik, F. Meier, G.R. Snow

University of Nebraska–Lincoln, Lincoln, USA

J. Dolen, A. Godshalk, I. Iashvili, A. Kharchilava, A. Kumar, S. Rappoccio

State University of New York at Buffalo, Buffalo, USA

G. Alverson, E. Barberis, D. Baumgartel, M. Chasco, J. Haley, A. Massironi, D.M. Morse, D. Nash, T. Orimoto, D. Trocino, D. Wood, J. Zhang

Northeastern University, Boston, USA

K.A. Hahn, A. Kubik, N. Mucia, N. Odell, B. Pollack, A. Pozdnyakov, M. Schmitt, S. Stoynev, K. Sung, M. Velasco, S. Won

Northwestern University, Evanston, USA

D. Berry, A. Brinkerhoff, K.M. Chan, A. Drozdetskiy, M. Hildreth, C. Jessop, D.J. Karmgard, N. Kellams, K. Lannon, W. Luo, S. Lynch, N. Marinelli, T. Pearson, M. Planer, R. Ruchti, N. Valls, M. Wayne, M. Wolf, A. Woodard

University of Notre Dame, Notre Dame, USA

L. Antonelli, B. Bylsma, L.S. Durkin, S. Flowers, C. Hill, R. Hughes, K. Kotov, T.Y. Ling, D. Puigh, M. Rodenburg, G. Smith, C. Vuosalo, B.L. Winer, H. Wolfe, H.W. Wulsin

The Ohio State University, Columbus, USA

E. Berry, P. Elmer, P. Hebda, A. Hunt, S.A. Koay, P. Lujan, D. Marlow, T. Medvedeva, M. Mooney, J. Olsen, P. Piroué, X. Quan, H. Saka, D. Stickland, C. Tully, J.S. Werner, S.C. Zenz, A. Zuranski

Princeton University, Princeton, USA

E. Brownson, H. Mendez, J.E. Ramirez Vargas

University of Puerto Rico, Mayaguez, USA

E. Alagoz, V.E. Barnes, D. Benedetti, G. Bolla, D. Bortoletto, M. De Mattia, A. Everett, Z. Hu, M.K. Jha, M. Jones, K. Jung, M. Kress, N. Leonardo, D. Lopes Pegna, V. Maroussov, P. Merkel, D.H. Miller, N. Neumeister, B.C. Radburn-Smith, I. Shipsey, D. Silvers, A. Svyatkovskiy, F. Wang, W. Xie, L. Xu, H.D. Yoo, J. Zablocki, Y. Zheng

Purdue University, West Lafayette, USA

N. Parashar, J. Stupak

Purdue University Calumet, Hammond, USA

A. Adair, B. Akgun, K.M. Ecklund, F.J.M. Geurts, W. Li, B. Michlin, B.P. Padley, R. Redjimi, J. Roberts, J. Zabel

Rice University, Houston, USA

B. Betchart, A. Bodek, R. Covarelli, P. de Barbaro, R. Demina, Y. Eshaq, T. Ferbel, A. Garcia-Bellido, P. Goldenzweig, J. Han, A. Harel, D.C. Miner, G. Petrillo, D. Vishnevskiy

University of Rochester, Rochester, USA

R. Ciesielski, L. Demortier, K. Goulianos, G. Lungu, C. Mesropian

The Rockefeller University, New York, USA

S. Arora, A. Barker, J.P. Chou, C. Contreras-Campana, E. Contreras-Campana, D. Duggan, D. Ferencek, Y. Gershtein, R. Gray, E. Halkiadakis, D. Hidas, A. Lath, S. Panwalkar, M. Park, R. Patel, V. Rekovic, S. Salur, S. Schnetzer, C. Seitz, S. Somalwar, R. Stone, S. Thomas, P. Thomassen, M. Walker

Rutgers, The State University of New Jersey, Piscataway, USA

K. Rose, S. Spanier, A. York

University of Tennessee, Knoxville, USA

O. Bouhali [56], R. Eusebi, W. Flanagan, J. Gilmore, T. Kamon [57], V. Khotilovich, V. Krutelyov, R. Montalvo, I. Osipenkov, Y. Pakhotin, A. Perloff, J. Roe, A. Rose, A. Safonov, T. Sakuma, I. Suarez, A. Tatarinov

Texas A&M University, College Station, USA

N. Akchurin, C. Cowden, J. Damgov, C. Dragoiu, P.R. Dudero, J. Faulkner, K. Kovitanggoon, S. Kunori, S.W. Lee, T. Libeiro, I. Volobouev

Texas Tech University, Lubbock, USA

E. Appelt, A.G. Delannoy, S. Greene, A. Gurrola, W. Johns, C. Maguire, Y. Mao, A. Melo, M. Sharma, P. Sheldon, B. Snook, S. Tuo, J. Velkovska

Vanderbilt University, Nashville, USA

M.W. Arenton, S. Boutle, B. Cox, B. Francis, J. Goodell, R. Hirosky, A. Ledovskoy, H. Li, C. Lin, C. Neu, J. Wood

University of Virginia, Charlottesville, USA

S. Gollapinni, R. Harr, P.E. Karchin, C. Kottachchi Kankanamge Don, P. Lamichhane

Wayne State University, Detroit, USA

D.A. Belknap, D. Carlsmith, M. Cepeda, S. Dasu, S. Duric, E. Friis, R. Hall-Wilton, M. Herndon, A. Hervé, P. Klabbers, J. Klukas, A. Lanaro, C. Lazaridis, A. Levine, R. Loveless, A. Mohapatra, I. Ojalvo, T. Perry, G.A. Pierro, G. Polese, I. Ross, T. Sarangi, A. Savin, W.H. Smith, N. Woods

University of Wisconsin, Madison, USA

† Deceased.
1 Also at Vienna University of Technology, Vienna, Austria.
2 Also at CERN, European Organization for Nuclear Research, Geneva, Switzerland.
3 Also at Institut Pluridisciplinaire Hubert Curien, Université de Strasbourg, Université de Haute Alsace Mulhouse, CNRS/IN2P3, Strasbourg, France.
4 Also at National Institute of Chemical Physics and Biophysics, Tallinn, Estonia.
5 Also at Skobeltsyn Institute of Nuclear Physics, Lomonosov Moscow State University, Moscow, Russia.
6 Also at Universidade Estadual de Campinas, Campinas, Brazil.
7 Also at California Institute of Technology, Pasadena, USA.
8 Also at Laboratoire Leprince-Ringuet, Ecole Polytechnique, IN2P3–CNRS, Palaiseau, France.

[9] Also at Suez University, Suez, Egypt.
[10] Also at Cairo University, Cairo, Egypt.
[11] Also at Fayoum University, El-Fayoum, Egypt.
[12] Also at British University in Egypt, Cairo, Egypt.
[13] Now at Ain Shams University, Cairo, Egypt.
[14] Also at Université de Haute Alsace, Mulhouse, France.
[15] Also at Joint Institute for Nuclear Research, Dubna, Russia.
[16] Also at Brandenburg University of Technology, Cottbus, Germany.
[17] Also at The University of Kansas, Lawrence, USA.
[18] Also at Institute of Nuclear Research ATOMKI, Debrecen, Hungary.
[19] Also at Eötvös Loránd University, Budapest, Hungary.
[20] Also at University of Debrecen, Debrecen, Hungary.
[21] Also at Tata Institute of Fundamental Research – HECR, Mumbai, India.
[22] Now at King Abdulaziz University, Jeddah, Saudi Arabia.
[23] Also at University of Visva-Bharati, Santiniketan, India.
[24] Also at University of Ruhuna, Matara, Sri Lanka.
[25] Also at Isfahan University of Technology, Isfahan, Iran.
[26] Also at Sharif University of Technology, Tehran, Iran.
[27] Also at Plasma Physics Research Center, Science and Research Branch, Islamic Azad University, Tehran, Iran.
[28] Also at Università degli Studi di Siena, Siena, Italy.
[29] Also at Centre National de la Recherche Scientifique (CNRS) – IN2P3, Paris, France.
[30] Also at Purdue University, West Lafayette, USA.
[31] Also at Universidad Michoacana de San Nicolas de Hidalgo, Morelia, Mexico.
[32] Also at National Centre for Nuclear Research, Swierk, Poland.
[33] Also at Institute for Nuclear Research, Moscow, Russia.
[34] Also at St. Petersburg State Polytechnical University, St. Petersburg, Russia.
[35] Also at Faculty of Physics, University of Belgrade, Belgrade, Serbia.
[36] Also at Facoltà Ingegneria, Università di Roma, Roma, Italy.
[37] Also at Scuola Normale e Sezione dell'INFN, Pisa, Italy.
[38] Also at University of Athens, Athens, Greece.
[39] Also at Paul Scherrer Institut, Villigen, Switzerland.
[40] Also at Institute for Theoretical and Experimental Physics, Moscow, Russia.
[41] Also at Albert Einstein Center for Fundamental Physics, Bern, Switzerland.
[42] Also at Gaziosmanpasa University, Tokat, Turkey.
[43] Also at Adiyaman University, Adiyaman, Turkey.
[44] Also at Cag University, Mersin, Turkey.
[45] Also at Mersin University, Mersin, Turkey.
[46] Also at Izmir Institute of Technology, Izmir, Turkey.
[47] Also at Ozyegin University, Istanbul, Turkey.
[48] Also at Kafkas University, Kars, Turkey.
[49] Also at Mimar Sinan University, Istanbul, Istanbul, Turkey.
[50] Also at Rutherford Appleton Laboratory, Didcot, United Kingdom.
[51] Also at School of Physics and Astronomy, University of Southampton, Southampton, United Kingdom.
[52] Also at University of Belgrade, Faculty of Physics and Vinca Institute of Nuclear Sciences, Belgrade, Serbia.
[53] Also at Argonne National Laboratory, Argonne, USA.
[54] Also at Erzincan University, Erzincan, Turkey.
[55] Also at Yildiz Technical University, Istanbul, Turkey.
[56] Also at Texas A&M University at Qatar, Doha, Qatar.
[57] Also at Kyungpook National University, Daegu, Republic of Korea.